PHYSICAL REVIEW D **81,** 044017 (2010)

Black hole in the expanding universe from intersecting branes

Kei-ichi Maeda[1,2,*] and Masato Nozawa[1,*]

[1]*Department of Physics, Waseda University, Okubo 3-4-1, Shinjuku, Tokyo 169-8555, Japan*
[2]*Waseda Research Institute for Science and Engineering, Okubo 3-4-1, Shinjuku, Tokyo 169-8555, Japan*
(Received 21 December 2009; published 10 February 2010)

We study physical properties and global structures of a time-dependent, spherically symmetric solution obtained via the dimensional reduction of intersecting M-branes. We find that the spacetime describes a maximally charged black hole which asymptotically tends to the Friedmann-Lemaître-Robertson-Walker universe filled by a stiff matter. The metric solves the field equations of the Einstein-Maxwell-dilaton system, in which four Abelian gauge fields couple to the dilation with different coupling constants. The spacetime satisfies the dominant energy condition and is characterized by two parameters, Q and τ, related to the Maxwell charge and the relative ratio of black-hole horizon radii, respectively. In spite of the nontrivial time dependence of the metric, it turns out that the black-hole event horizon is a Killing horizon. This unexpected symmetry may be ascribed to the fact that the 11-dimensional brane configurations are supersymmetric in the static limit. Finally, combining with laws of the trapping horizon, we discuss the thermodynamic properties of the black hole. It is shown that the horizon possesses a nonvanishing temperature, contrary to the extremal Reissner-Nordström solution.

DOI: 10.1103/PhysRevD.81.044017 PACS numbers: 04.70.Bw, 04.50.−h, 04.50.Gh

I. INTRODUCTION

Brane configurations in string/M theory have offered a new avenue for producing wide classes of solutions of physical interest in lower dimensions. The attempts of an early date have mainly aimed at the construction of various kinds of black holes [1–4] via the Kaluza-Klein compactification of (intersecting) branes [5–9]. An interesting application of this idea is to dynamically realize our 4D universe by incorporating time dependence [10–12]. An alternate mechanism that provides lower-dimensional spacetimes is the brane world [13,14], in which our 4D world is regarded as the hypersurface embedded in the bulk. Cosmological evolutionary scenarios based on the dynamically moving brane or colliding branes give a significant modification from the standard cosmology in high energy regime, still consistent with the present day observations [15–17].

One can extend these studies further into the case where the brane involves a nontrivial space- and time-coordinate dependence. Correspondingly, the 4D reduced solution becomes spatially inhomogeneous and evolving in time. A preliminary result was presented in [18], where colliding D3 branes were discussed within the framework of type IIB supergravity (see [19] for analysis of the Hořawa-Witten domain wall). Lower-dimensional solutions obtained by compactifying extended directions of these moving branes or dynamically intersecting branes have much richer properties than those obtained from static counterparts. Recently, the authors of [20] studied dynamical solutions describing intersecting branes in more general settings and obtained a number of intriguing solutions with wide potential applications. Among other things, their tantalizing findings are the ''cosmological black holes'' in the expanding Friedmann-Lemaître-Robertson-Walker (FLRW) universe, that is, black holes in a nonisolated system which asymptotically approaches the homogeneous and isotropic cosmology. In this paper, we are concerned with this ''candidate'' black-hole spacetime obtained in [20].

Studies of black holes in our universe have been primarily focused on the stationary spacetimes in the literature [21]. Such approaches are definitely the first step because we can anticipate that dynamic variations will die away and the system will settle down to equilibrium states if a sufficiently long time has passed after the formation of a black hole. A number of physical properties of stationary black holes have been elucidated by many people. Specifically, the black-hole uniqueness theorem in stationary spacetime is the major triumph of mathematical relativity and established that the Kerr solution describes all vacuum black holes in isolated systems [21]. An essential crux toward the uniqueness proof is the demonstration that the event horizon in stationary spacetime is a Killing horizon [22]. Since a Killing horizon is a null surface to which the Killing vector is normal, we can identify the locus of a black hole simply by the local spacetime symmetry. Furthermore, it has been revealed that Killing horizons admit three laws of black-hole mechanics which bear an amazing resemblance to ordinary thermodynamics [23–30]. This implies a deep association between classical gravity, statistical physics, and quantum mechanics, so that black-hole thermodynamics is expected to have a key role in understanding quantum aspects of gravity. A notable progression in string theory is the microscopic derivation of black-hole entropy in the perspective of intersecting brane configurations [2,3].

*maeda@waseda.jp
†nozawa@gravity.phys.waseda.ac.jp

If we get rid of the stationarity assumptions to discuss dynamics, the uniqueness theorem no longer holds. Accordingly, a variety of black-hole solutions are likely to exist. However, very little is known concerning the exact solutions of Einstein's equations that describe growing black holes interplaying with surroundings. A novel aspect of a nonisolated system is that it generally possesses a time dependence and need not be asymptotically flat. The background fluid distributions filling the universe become inhomogeneous due to the presence of the black hole, while the black hole grows by swallowing the ambient matters. Such a complexity has rendered the system considerably elusive.

A large amount of effort has been devoted thus far to attempt to obtain black holes in the FLRW universe. An initiated work is the simplest model invented by Einstein and Straus [31], which is often referred to as a ''Swiss-cheese Universe.'' They matched the Schwarzschild solution with an FLRW universe by means of a ''cut and paste'' method. So the black-hole part metric still maintains a time symmetry, and then it appears that this model does not capture a realistic situation of the dynamic phase. If there is a positive cosmological constant, we have the Schwarzschild–de Sitter (SdS) or the Reissner–Nordström–de Sitter (RNdS) solution [21,32]. Those spacetimes can be redescribed by the coordinate transformation in the form of a black hole in the exponentially expanding universe [33]. However they have a ''timelike'' Killing vector and are essentially static.

In recent years, Sultana and Dyer have constructed a more sophisticated black-hole solution in a dynamical background by a conformal technique [34]. The matter content is composed of null dust and usual dust fluids, and the solution tends to an Einstein–de Sitter spacetime asymptotically. This model, however, suffers from the issue of violating energy conditions: energy densities of both fluids become negative at late times.

One of the other widely known black-hole candidates in the FLRW universe is the McVittie solution [35], which is a spherically symmetric, expanding solution of the Einstein equations sourced by a perfect fluid. Taking asymptotic limits, the solution looks like an FLRW universe at ''infinity,'' and like a black hole near the ''horizon,'' hence one might be led to conclude that the McVittie spacetime might describe a black hole in the expanding FLRW universe. Attractive as this might be, however, such an optimistic outlook would jump to a hasty conclusion. As asserted in [36], the McVittie solution is disqualified as a black hole in an FLRW universe. Since our spacetime metric is in appearance quite similar to the McVittie solution in several respects, the above concrete example motivates us to explore the global structure of time-dependent black holes with enough care. In this paper, we intend to provide a comprehensive account of the global picture of dynamical solutions obtained in [20].

Another interesting issue of a time-dependent spacetime containing black holes is the collision of black holes. Kastor and Traschen found the collection of extremely charged black holes in the de Sitter universe and discussed their collision [37,38]. This solution is a time-dependent generalization of its celebrated cousin, the Majumbdar-Papapetrou solution, which describes extremely charged Reissner-Nordstrøm (RN) black holes [39]. In spite of the lack of Bogomol'nyi-Prasad-Sommerfeld (BPS) states for $\Lambda > 0$, it is somewhat astonishing that the superposition of RNdS black holes is possible. The same situation happens in our spacetime obtained by the time-dependent intersecting brane system in which no BPS states are preserved. Making use of this exact solution, we can discuss the collision of black holes in the power-law contracting universe just as the brane collision [18].

The plan of the rest of the paper is as follows. We shall begin by reviewing the dynamical ''black-hole solution'' derived in [20]. Section III involves a detailed examination about the properties of matter fields. Our main result is contained in Sec. IV, where we will elucidate spacetime structures based on local and global perspectives. In Sec. V we draw the conformal diagram that allows us to pictorially identify a black hole embedded in an expanding universe. Section VI summarizes our conclusive results with several future outlooks. In order to keep the mainstream of the text, we relegate some issues to Appendixes.

We shall work in the units of $c = \hbar = 1$ and retain the gravitational constant $\kappa^2 = 8\pi G$. We pertain to the notation R to denote the circumference radius, so that we use the script throughout the paper for the spacetime curvature $\mathcal{R}^{\mu}{}_{\nu\rho\sigma}V^{\nu} := 2\nabla_{[\rho}\nabla_{\sigma]}V^{\mu}$, $\mathcal{R}_{\mu\nu} := \mathcal{R}^{\rho}{}_{\mu\rho\nu}$, and $\mathcal{R} := \mathcal{R}^{\mu}{}_{\mu}$.

II. TIME-DEPENDENT SOLUTIONS FROM THE INTERSECTING BRANE SYSTEM

The authors of [20] have classified the possible time-dependent intersecting brane systems in M theory by assuming the metric form and presented some interesting solutions in lower dimensions by compactification. Among other things, one of the most interesting solutions is a ''black hole'' in the expanding universe. In the case where all branes are at rest, i.e., spacetime is static, the 4D reduced solution indeed describes a black hole, which is obtained from the M2-M2-M5-M5 brane system (four brane charges) or from the M2-M5-W-KK brane system (two brane charges plus a Brinkmann wave and a Kaluza-Klein monopole). The 5D black-hole solution is similarly derived from the M2-M2-M2 brane system (three brane charges) or from the M2-M5-W brane system (two branes plus a Brinkmann wave). Time-dependent extensions of those lower-dimensional solutions are produced from the dynamical intersecting brane systems, in which only a single brane is time dependent [20]. These 11D solutions

and the procedure of the dimensional reduction are shortly summarized in Appendix A.

After the toroidal compactification of 11D intersecting brane solutions, we have a 4D black-hole solution, which is spherically symmetric, time, and radial coordinate dependent (we relegate the extension into the case of nonspherical, multiple black holes to Appendix B). The 4D metric in the Einstein frame is given by

$$ds^2 = -\Xi dt^2 + \frac{1}{\Xi}(dr^2 + r^2 d\Omega_2^2), \tag{2.1}$$

with

$$\Xi = \left[\left(\frac{t}{t_0} + \frac{Q_T}{r}\right)\left(1 + \frac{Q_S}{r}\right)\left(1 + \frac{Q_{S'}}{r}\right)\left(1 + \frac{Q_{S''}}{r}\right)\right]^{-1/2}, \tag{2.2}$$

where $d\Omega_2^2 = d\theta^2 + \sin^2\theta d\phi^2$ denotes the line element of a unit round two-sphere. The constants Q_T and Q_S, $Q_{S'}$, $Q_{S''}$ are charges of one time-dependent brane and three static branes, respectively. Here and hereafter, T and S are understood to trace their origin to time-dependent and static branes. The above metric manifests that the conditions of stationarity and asymptotic flatness were both relaxed.

Assuming $t/t_0 > 0$ and changing to the new time slice $\bar{t}$ defined by

$$\frac{\bar{t}}{\bar{t}_0} = \left(\frac{t}{t_0}\right)^{3/4} \quad \text{with} \quad \bar{t}_0 = \frac{4}{3}t_0, \tag{2.3}$$

we are able to put the solution (2.1) into a more suggestive form,

$$ds^2 = -\bar{\Xi} d\bar{t}^2 + \frac{a^2}{\bar{\Xi}}(dr^2 + r^2 d\Omega_2^2), \tag{2.4}$$

where

$$\bar{\Xi} = \left[\left(1 + \frac{Q_T}{a^4 r}\right)\left(1 + \frac{Q_S}{r}\right)\left(1 + \frac{Q_{S'}}{r}\right)\left(1 + \frac{Q_{S''}}{r}\right)\right]^{-1/2}, \tag{2.5}$$

and

$$a = \left(\frac{\bar{t}}{\bar{t}_0}\right)^{1/3}. \tag{2.6}$$

When we take the limit of $r \to \infty$, we can find that the metric (2.4) asymptotically tends to a flat FLRW spacetime,

$$ds^2 = -d\bar{t}^2 + a^2(dr^2 + r^2 d\Omega_2^2). \tag{2.7}$$

Here, the scale factor expands as $a \propto \bar{t}^{1/3}$, which is the same as the expansion law of the universe filled by a stiff matter. Hence we expect that this spacetime is an asymptotically FLRW universe with the equation of state $P = \rho$.

On the other hand, taking the limit $r \to 0$ with t being finite, the time dependence turns off and the metric (2.4) reduces to the direct product of 2D anti–de Sitter (AdS_2) space with round sphere,

$$ds^2 = -\frac{r^2}{\bar{Q}^2} dt^2 + \frac{\bar{Q}^2}{r^2}(dr^2 + r^2 d\Omega_2^2), \tag{2.8}$$

where $\bar{Q} := (Q_T Q_S Q_{S'} Q_{S''})^{1/4}$ plays the role of curvature radii of AdS_2 and S_2. This is a typical "throat" geometry of an extreme black hole. To take the case of an extreme RN spacetime with the Arnowitt-Deser-Misner (ADM) mass $M = \bar{Q}$, the metric in the isotropic coordinates reads

$$ds^2 = -\left(1 + \frac{\bar{Q}}{r}\right)^{-2} dt^2 + \left(1 + \frac{\bar{Q}}{r}\right)^2 (dr^2 + r^2 d\Omega_2^2), \tag{2.9}$$

which indeed asymptotes to the spacetime (2.8) in the limit $r \to 0$ with t kept finite.[1] Thus, we may speculate that there might exist a degenerate event horizon at $r = 0$.

For the reason stated above, it might be tempting to regard the present spacetime (2.1) as a degenerate black hole with radius $\bar{Q}$ residing at the center $r = 0$ of the expanding FLRW universe. However, there is *a prioi* no guarantee that the global picture of the solution is obtainable simply from the asymptotic considerations, just as we inferred the causal structure of the Schwarzschild-AdS spacetime from those of the Schwarzschild and the AdS metrics. Furthermore, it is far from clear to what extent the spacetime shares the physical properties as its limiting counterparts. In fact, a more detailed argument casts doubt on the above naïve expectation.

To see this, it is instructive to consider the McVittie spacetime [35],

$$ds^2 = -\left(\frac{1 - M/2ar}{1 + M/2ar}\right)^2 dt^2 + a^2\left(1 + \frac{M}{2ar}\right)^4 (dr^2 + r^2 d\Omega_2^2), \tag{2.10}$$

where $a = a(t)$. The metric (2.4) with (2.5) and (2.6) looks quite similar to the McVittie spacetime in appearance. In the limit of $r \to \infty$, the McVittie spacetime asymptotes to the flat FLRW universe with the scale factor a. If a is set to be constant ($a \equiv 1$), we recover the Schwarzschild spacetime with the ADM mass M written in the isotropic coordinates. So one might deduce that the McVittie spacetime (2.10) describes a black hole immersed in the FLRW universe.

[1] It should be emphasized that the $AdS_2 \times S_2$ geometry (2.8) indeed approximates the whole portion of the near-horizon geometry—the three-dimensional null surface—of an extremal RN solution (and more generally, of any kinds of an extremal black hole [40]), not restricted to the throat. To the contrary, the spacetime (2.8) fails to describe the near-horizon geometry of the event horizon of our time-dependent solution. As proof of the incident, we will show in a later section that the temperature of a dynamical black hole does not vanish in the present case, unlike the extremal RN black hole having a zero Hawking temperature.

However, it turns out that this exemplifies the fact that our naïve estimate ceases to be true.[2] When the scale factor obeys the power-law form $a \propto t^p (p > 0)$, a curvature singularity appears at $r = M/(2a)$. As Nolan pointed out [36], the spacetime events described by $r = M/(2a)$ in part consist of a shell-crossing spacelike singularity lying a future of a big-bang singularity $a = 0$. The surface $r = M/(2a)$ fails to describe a (regular) horizon of a black hole in the FLRW universe. Inferring from the ''monopole term'' m/r, does this spacetime instead describe a point mass (singularity) at $r = 0$ embedded in the expanding universe? The answer is no. It turns out that $r = 0$ corresponds to infinity, rather than the locus of a point particle in the universe. Besides that, according to the quasilocal definition of a horizon, the McVittie spacetime may serve as a ''white hole'' in an expanding FLRW universe. As a good lesson, we are required to take special care to conclude what the present spacetime describes.

In this paper, we study the above spacetime (2.1) more thoroughly [we are working mainly in Eq. (2.1) rather than Eq. (2.4), because the former coordinates cover a wider range than the latter]. We assume $t_0 > 0$, viz., the background universe is expanding. For simplicity and definiteness of our argument, we will specialize to the case in which all charges are equal, i.e., $Q_T = Q_S = Q_{S'} = Q_{S''} \equiv Q(>0)$.[3] To be specific, we will analyze the spacetime metric

$$ds^2 = -\Xi dt^2 + \Xi^{-1}(dr^2 + r^2 d\Omega_2^2), \tag{2.11}$$

whose component Ξ, Eq. (2.2), is simplified to

$$\Xi = (H_T H_S^3)^{-1/2}, \tag{2.12}$$

with

$$H_T = \frac{t}{t_0} + \frac{Q}{r}, \qquad H_S = 1 + \frac{Q}{r}. \tag{2.13}$$

A more general background with distinct charges is yet to be investigated. The result for the 5D solution will be given in Appendix C.

III. MATTER FIELDS AND THEIR PROPERTIES

It is a good starting point to draw attention toward the matter fields. Since we know explicitly the 4D metric components, we can read off the total energy-momentum tensor of matter fluid(s) from the 4D Einstein equations,

$$\kappa^2 T_{\mu\nu} = \mathcal{G}_{\mu\nu}, \tag{3.1}$$

where $\mathcal{G}_{\mu\nu} = \mathcal{R}_{\mu\nu} - (\mathcal{R}/2) g_{\mu\nu}$ is the Einstein tensor. What kind of matter fluids can we expect? There may appear at least two fluid components: one is a scalar field and the other is a U(1) gauge field. This is because we compactify seven spaces and we have originally a 4-form field in 11D supergravity theory. The torus compactification gives a set of scalar fields and the 4-form field behaves as a U(1) gauge field in 4D. In our solution, we assume four branes, which give rise to four U(1) gauge fields.

As shown in Appendix A, we can derive the following effective 4D action from the 11D supergravity solution via compactification,

$$\mathcal{S} = \int d^4x\sqrt{-g}\Big[\frac{1}{2\kappa^2}\mathcal{R} - \frac{1}{2}(\nabla\Phi)^2 - \frac{1}{16\pi}\sum_A e^{\lambda_A \kappa\Phi}(F^{(A)}_{\mu\nu})^2\Big], \tag{3.2}$$

where Φ, $F^{(A)}_{\mu\nu}$, and λ_A ($A = T, S, S', S''$) are a scalar field, four U(1) fields, and coupling constants, respectively.

The above action yields the following set of basic equations:

$$\mathcal{G}_{\mu\nu} = \kappa^2(T^{(\Phi)}_{\mu\nu} + T^{(\mathrm{em})}_{\mu\nu}), \tag{3.3}$$

$$\Box\Phi - \frac{\kappa}{16\pi}\sum_A \lambda_A e^{\lambda_A\kappa\Phi}(F^{(A)}_{\mu\nu})^2 = 0, \tag{3.4}$$

$$\nabla^\nu(e^{\lambda_A\kappa\Phi}F^{(A)}_{\mu\nu}) = 0, \tag{3.5}$$

where

$$T^{(\Phi)}_{\mu\nu} = \nabla_\mu\Phi\nabla_\nu\Phi - \tfrac{1}{2}g_{\mu\nu}(\nabla\Phi)^2, \tag{3.6}$$

$$T^{(\mathrm{em})}_{\mu\nu} = \frac{1}{4\pi}\sum_A e^{\lambda_A\kappa\Phi}\Big[F^{(A)}_{\mu\rho}F^{(A)\rho}_{\ \ \nu} - \frac{1}{4}g_{\mu\nu}(F^{(A)}_{\alpha\beta})^2\Big]. \tag{3.7}$$

For the present case with all the same charges, two different coupling constants appear.

A simple calculation shows that our spacetime metric (2.11) satisfies the above basic equations (3.3), (3.4), and (3.5), provided the dilaton profile

$$\kappa\Phi = \frac{\sqrt{6}}{4}\ln\Big(\frac{H_T}{H_S}\Big), \tag{3.8}$$

and four electric gauge fields

$$\kappa F^{(T)}_{01} = -\frac{\sqrt{2\pi}Q}{r^2H_T^2}, \qquad \kappa F^{(S)}_{01} = \kappa F^{(S')}_{01} = \kappa F^{(S'')}_{01} = -\frac{\sqrt{2\pi}Q}{r^2H_S^2}, \tag{3.9}$$

with the coupling constants

[2]The case $a = e^{Ht}$ with constant H is exceptional for which the metric describes an SdS spacetime. But we are reluctant to refer to this as a black hole in the expanding universe, since the metric is rewritten in a static form thanks to Birkhoff's theorem.

[3]If Q_T is different from the other three same charges Q_S, the present result still holds. It is because such a difference amounts to the trivial conformal change $ds^2 = (Q_T/Q_S)^{1/2}[-\Xi_* dt_*^2 + \Xi_*^{-1}(dr^2 + d\Omega_2^2)]$, with simple parameter redefinitions: $\Xi_* = [(t_*/t_{*0} + Q_S/r)(1 + Q_S/r)^3]^{-1/2}$, $t_* = (Q_T/Q_S)^{-1/2}t$, and $t_{*0} = (Q_T/Q_S)^{1/2}t_0$.

$$\lambda_T = \sqrt{6}, \qquad \lambda_S \equiv \lambda_{S'} \equiv \lambda_{S''} = -\sqrt{6}/3. \tag{3.10}$$

The U(1) fields are expressed in terms of the electrostatic potentials $F^{(A)}_{\mu\nu} = \nabla_\mu A^{(A)}_\nu - \nabla_\nu A^{(A)}_\mu$ as

$$\kappa A^{(T)}_0 = \frac{\sqrt{2\pi}}{H_T}, \qquad \kappa A^{(S)}_0 = \sqrt{2\pi}\left(\frac{1}{H_S} - 1\right), \tag{3.11}$$

where we have tuned $A^{(S)}_0$ to assure $A^{(S)}_0 \to 0$ as $r \to \infty$ using a gauge freedom. Therefore the present spacetime (2.11) is the exact solution of the Einstein-Maxwell-dilaton system (3.2).

One may verify that Q is the (electric) charge satisfying

$$\frac{Q}{\sqrt{G}} = \frac{1}{4\pi}\int_S e^{\lambda_A \kappa \Phi} F^{(A)}_{\mu\nu} dS^{\mu\nu}, \tag{3.12}$$

where S is a round sphere surrounding the source. This expression is obtainable by the first integral of Eq. (3.5).

Note that one can also find a magnetically charged solution instead of (3.9). However, this can be realized by a duality transformation

$$\Phi \to -\Phi, \qquad F^{(A)}_{\mu\nu} \to \tfrac{1}{2} e^{\lambda_A \kappa \Phi} \epsilon_{\mu\nu\rho\sigma} F^{(A)\rho\sigma}, \tag{3.13}$$

which is a symmetry involved in the action (3.2). Henceforth, we will make our attention only to the electrically charged case. This restriction does not affect the global spacetime picture.

A. Energy density and pressure

Using our solution (2.1), we can evaluate the components of the energy-momentum tensors, i.e., the energy density and pressures for each field [the dilaton Φ and U(1) fields $F^{(A)}_{\mu\nu}$]. They are given by

$$\begin{aligned}\rho^{(\Phi)} = P^{(\Phi)}_r &= \frac{1}{2}(\Xi^{-1}\dot{\Phi}^2 + \Xi\Phi'^2) \\ &= \frac{3}{16\kappa^2}\left[\frac{1}{t_0^2}\left(\frac{H_S}{H_T}\right)^{3/2} + \frac{Q^2}{r^4}\frac{(H_T - H_S)^2}{(H_T^5 H_S^7)^{1/2}}\right] > 0,\end{aligned} \tag{3.14}$$

$$\begin{aligned}P^{(\Phi)}_\theta = P^{(\Phi)}_\phi &= \frac{1}{2}(\Xi^{-1}\dot{\Phi}^2 - \Xi\Phi'^2) \\ &= \frac{3}{16\kappa^2}\left[\frac{1}{t_0^2}\left(\frac{H_S}{H_T}\right)^{3/2} - \frac{Q^2}{r^4}\frac{(H_T - H_S)^2}{(H_T^5 H_S^7)^{1/2}}\right],\end{aligned} \tag{3.15}$$

$$\begin{aligned}\rho^{(\mathrm{em})} = -P^{(\mathrm{em})}_r &= P^{(\mathrm{em})}_\theta = P^{(\mathrm{em})}_\phi \\ &= \frac{1}{8\pi}[e^{\lambda_T \kappa\Phi}(F^{(T)}_{01})^2 + 3e^{\lambda_S\kappa\Phi}(F^{(S)}_{01})^2], \\ &= \frac{Q^2}{4\kappa^2 r^4}\left[\frac{1}{H_T^4}\left(\frac{H_T}{H_S}\right)^{3/2} + \frac{3}{H_S^4}\left(\frac{H_T}{H_S}\right)^{-1/2}\right] > 0.\end{aligned} \tag{3.16}$$

The time $t = t_0$ is special at which the energy density of the scalar field is uniform $\kappa^2\rho^{(\Phi)}(t_0) = 3/(16t_0^2)$, and soon after it becomes gradually inhomogeneous. We shall refer to t_0 as the *fiducial time*. As the universe expands, the energy density of the scalar field at infinity behaves $\rho^{(\Phi)} \propto t^{-3/2} \propto \bar{t}^{-2} \propto a^{-6}$, as expected for the FLRW universe with stiff matter or a massless scalar field. The energy density of the U(1) fields evaluated at the fiducial time is $\kappa^2\rho^{(\mathrm{em})}(t_0) = Q^2/(rH_S)^4 = Q^2/(r+Q)^4$, which is the same as that of the extreme RN spacetime, and decreases in time as $\kappa^2\rho^{(\mathrm{em})}(t, r) \propto t^{-1/2} \propto \bar{t}^{-2/3} \propto a^{-2}$ near infinity as in the same manner for the FLRW universe.

We can also find the energy flux $J^\mu := T^{\hat{0}\mu}$ whose spatial component $\mathcal{F}$ is given by

$$\kappa^2\mathcal{F} = \kappa^2 T^{\hat{0}}{}_{\hat{1}} = \kappa^2 T^{(\Phi)\hat{0}}{}_{\hat{1}} = -\frac{3Q}{8t_0}\frac{(H_T - H_S)}{r^2 H_T^2 H_S}, \tag{3.17}$$

where a hat denotes the tetrad component. Only the scalar field contributes to the energy flux, since no magnetic fields exist, i.e., no Poynting flux. One can find that the $\mathcal{F}$ becomes negative for $t > t_0$, implying that the scalar field energy is falling toward the black hole. However, as it turns out later, the flux never gets into the black hole. This may be attributed to the fact that the repulsive force caused by the U(1) fields becomes strong near the horizon and finely balances the attractive gravitational force of the dilaton field.

It is worthwhile here to discuss the issue of the energy conditions. Many candidates of black-hole solutions in an expanding universe found in the literature (McVittie's solution [35], Sultana-Dyer solution [34], etc.) do not respect energy conditions in the whole of spacetime. Now the present system—U(1) gauge fields coupled to a dilaton—apparently satisfies the energy condition and hence it provides us a nontrivial example. We may verify this explicitly as follows. Inspecting Eqs. (3.14), (3.15), and (3.16), we notice $\rho^{(\Phi)} = P^{(\Phi)}_r \geq P^{(\Phi)}_\theta$ and $\rho^{(\mathrm{em})} = -P^{(\mathrm{em})}_r \geq P^{(\mathrm{em})}_r$, from which we obtain

$$\begin{aligned}\rho &= \rho^{(\Phi)} + \rho^{(\mathrm{em})} = P^{(\Phi)}_r - P^{(\mathrm{em})}_r \geq P^{(\Phi)}_r + P^{(\mathrm{em})}_r = P_r, \\ \rho &= \rho^{(\Phi)} + \rho^{(\mathrm{em})} \geq P^{(\Phi)}_\theta + P^{(\mathrm{em})}_\theta = P_\theta,\end{aligned} \tag{3.18}$$

and

$$\begin{aligned}\rho + P_r &= (\rho^{(\Phi)} + P^{(\Phi)}_r) + (\rho^{(\mathrm{em})} + P^{(\mathrm{em})}_r) > 0, \\ \rho + P_\theta &= (\rho^{(\Phi)} + P^{(\Phi)}_\theta) + (\rho^{(\mathrm{em})} + P^{(\mathrm{em})}_\theta) > 0.\end{aligned} \tag{3.19}$$

These equations mean that $\rho \geq |P_i|$ $(i = 1, 2, 3)$ is satisfied anywhere.

The energy flux $J^\mu = T^{\hat{0}\mu}$ satisfies

$$\begin{aligned}J^\mu J_\mu &= -\rho^2 + \mathcal{F}^2 \\ &= -(\rho^{(\mathrm{em})})^2 - 2\rho^{(\mathrm{em})}\rho^{(\Phi)} - (P^{(\Phi)}_\theta)^2 < 0,\end{aligned} \tag{3.20}$$

where we have used the relation $(\rho^{(\Phi)})^2 - \mathcal{F}^2 = (P^{(\Phi)}_\theta)^2$ at

the second equality. Hence, the energy current J^μ is a timelike vector everywhere. It then follows that the spacetime (2.1) satisfies the dominant energy condition [$\rho \geq |P_i|$ ($i = 1, 2, 3$) and J^μ is nonspacelike].

B. Misner-Sharp energy

Another useful quantity to characterize matter fields is the quasilocal energy, which is defined on the closed two-surfaces. If the spacetime has an SO(3) symmetry, we are able to give a physically satisfactory quasilocal energy introduced by Misner and Sharp [41].

The utility of spherical symmetry lies in the fact that we can covariantly employ the circumference radius,

$$R(t, r) := |r|\Xi^{-1/2} = |r|(H_T H_S^3)^{1/4}, \tag{3.21}$$

in terms of which the area of metric sphere is given by $4\pi R^2$. R is a geometrical quantity and has an invariant meaning. It is occasionally of great advantage, instead of the comoving coordinate r, to make use of R. Using the circumference radius, the Misner-Sharp quasilocal energy is defined by [41]

$$m(t, r) := \frac{4\pi R}{\kappa^2}[1 - g^{\mu\nu}(\nabla_\mu R)(\nabla_\nu R)]. \tag{3.22}$$

This quantity is a useful local measure to demonstrate geometric properties of spacetime [42–44]. The Misner-Sharp energy represents a mass energy contained inside the surface of radius R. Once the compact surface is specified, the Misner-Sharp mass is given without any ambiguity. Such a quasilocalization is possible because of spherical symmetry, in which no gravitational wave exists. By definition, it is characterized by geometric structure (metric components and its first derivatives) and does not require the premise of asymptotic structure of spacetime. So, it is considerably advantageous for the analysis of local spacetime structure.

Physical interpretation of the Misner-Sharp energy has been further backed by various desirable properties: it satisfies the first law of thermodynamics [45], it shows the properties of positivity and monotonicity under the dominant energy conditions, and it reduces to ADM mass in the asymptotically flat spatial infinity. Reference [43] reinterpreted it by the integral of a locally conserved energy current coming from the symplectic structure of spherical symmetry. One may find the superiority of the use of Misner-Sharp energy in the next section.

The present metric (2.11) with (2.13) gives rise to

$$\kappa^2 m = \frac{\pi|r|[r^2 H_T H_S^5 + 16 t_0^2 H_T^2 H_S^2 - (H_S t + 3H_T t_0)^2]}{4t_0^2 (H_T^7 H_S^5)^{1/4}}. \tag{3.23}$$

The physical meaning of each term in this equation is best understood at the fiducial time $t = t_0$, at which the Misner-Sharp mass is expressed as

$$\begin{aligned}\kappa^2 m(t_0, R) &= \frac{\pi(|r|H_S)^3}{4t_0^2} + 4\pi\frac{Q}{H_S} + 4\pi Q \\ &= \kappa^2\left(\frac{4\pi}{3}R^3\rho^{(\Phi)}(t_0) \right. \\ &\quad \left. + 4\pi\int_Q^R R^2 dR\rho^{(\mathrm{em})}(t_0, R)\right) + 4\pi Q.\end{aligned} \tag{3.24}$$

The first term corresponds to the energy of the scalar field, and the second and the last terms to the U(1) energies outside of and inside of the black hole, respectively.

If we set $Q = 0$, the second and third terms in Eq. (3.23) are combined to cancel, and m is expressed by the coordinates (2.4) as

$$m = \frac{ar^3}{2G}\left(\frac{da}{d\bar{t}}\right)^2 = \frac{4\pi}{3}(ar)^3\rho^{(\Phi)}, \tag{3.25}$$

as expected for the background FLRW universe. This also justifies the first term in (3.23) to be the contribution of the scalar field.

IV. SPACETIME STRUCTURE

Let us now turn to the main task of revealing spacetime structure of the solution (2.11). In order to address this issue, it is of significance to discuss the following:

(i) singularity,
(ii) trapped surface,
(iii) event horizon, and
(iv) asymptotic structure.

The first two topics are associated with the local character of spacetime, whereas the last two require global considerations. These are elementary issues to be explored in order to characterize the spacetime.

We wish to show that our metric (2.11) describes a black hole in the FLRW universe. To this end, we need to establish in the first place that the far outside region from the central inhomogeneous domain behaves nonpathologically. If the spacetime admits a naked singularity in the asymptotic region—other than the initial big-bang singularity—that is not covered by the event horizon, the solution would not gain popularity as a black hole.

According to a series of theorems due to Penrose and Hawking [22], the appearance of spacetime singularity is closely associated to the presence of trapped surfaces. Thus, the examination of the trapping property may provide us useful information of local spacetime geometry. In particular, we have two competing effects due to the black hole and the expanding cosmology: the former tends to focus light rays back into the hole while the latter tends to spread it out to infinity.

At first sight, one might expect to gain only a limited perception from the local point of view, even though the curvature singularity and local horizons are indeed of importance. Nevertheless, under physically reasonable cir-

cumstances, the existence of the local horizon implies that the event horizon lies outside it [22]. To be more precise, all trapped surfaces are contained within black holes under the null energy condition provided the spacetime is asymptotically flat with some additional technical assumptions (see Proposition 9.2.8 in [22] for the proof). So, this criterion is of use for our study.

In order to define a black hole as a "region of no escape," the spacetime must allow null infinity as an idealization of an observer sufficiently far in the distance from some central region. Thus the asymptotic analysis should also be emphasized. In particular, we will take a close look at null geodesic motions, since the null rays play a privileged role in the black-hole geometry. The above listed considerations are sufficient to provide us with insight into the global pictures of our dynamical spacetime (2.4).

In the remainder of this paper, we shall simplify our notations by using dimensionless variables $\tilde{t} := t/t_0$ and $\tilde{r} := r/Q$. The metric is also rewritten into dimensionless form $d\tilde{s}_4^2 = Q^{-2} ds_4^2$ as

$$d\tilde{s}_4^2 = -\tau^2 \tilde{\Xi} d\tilde{t}^2 + \tilde{\Xi}^{-1}(d\tilde{r}^2 + \tilde{r}^2 d\Omega_2^2), \tag{4.1}$$

with

$$\tau := \frac{t_0}{Q}, \qquad \tilde{\Xi} := \frac{\tilde{r}^2}{[(1+\tilde{t}\,\tilde{r})(1+\tilde{r})^3]^{1/2}}. \tag{4.2}$$

In this form, the metric involves only one dimensionless parameter $\tau = t_0/Q$, the physical meaning of which will be revealed below. We will affix a tilde to denote dimensionless quantities in what follows.

A. Singularity

The scalar curvature and the Kretschmann invariant scalar are given by

$$\begin{aligned}\mathcal{R} &= \kappa^2(P_\theta^{(\Phi)} + P_\phi^{(\Phi)}) \\ &= \frac{3}{8Q^2}\left[\frac{1}{\tau^2}\left(\frac{H_T}{H_S}\right)^{3/2} - \frac{1}{\tilde{r}^4}\frac{(H_T - H_S)^2}{(H_T^5 H_S^7)^{1/2}}\right],\end{aligned} \tag{4.3}$$

$$\begin{aligned}\mathcal{R}_{\mu\nu\rho\sigma}\mathcal{R}^{\mu\nu\rho\sigma} = \frac{1}{64\tau^4 Q^4 H_T^5 H_S^7}\Bigg[&15H_T^2 H_S^{10} + 6\left(\frac{\tau^2}{\tilde{r}^4}\right)H_T H_S^5(7H_T^2 + 10H_T H_S - H_S^2) + \left(\frac{\tau^4}{\tilde{r}^6}\right)\{9(31H_S^2 + 2H_S + 159)H_T^4 \\ &+ 12(7H_S^2 + 9H_S + 96)H_T^3 H_S + 6(15H_S^2 - 126H_S + 143)H_T^2 H_S^2 \\ &- 12(H_S - 1)(H_S + 15)H_T H_S^3 + 71(H_S - 1)^2 H_S^4\}\Bigg].\end{aligned} \tag{4.4}$$

These curvature invariants diverge when $H_T = 0$ and $H_S = 0$, that is, at

$$\tilde{t} = \tilde{t}_s(\tilde{r}) := -1/\tilde{r}, \quad \text{and} \quad \tilde{r} = -1. \tag{4.5}$$

At these spacetime points, the circumference radius R, Eq. (3.21), vanishes, i.e., they are central shell-focusing singularities. Thus, around infinity is free from singularities and is well behaved.

It deserves to observe the $\tilde{t} = 0$ surface, where the scale factor $a(\tilde{t})$ appearing in the metric (2.4) vanishes and is not singular at all since the curvature invariants remain finite therein. It follows that the big-bang singularity $\tilde{t} = 0$ is smoothed out due to a nonvanishing Maxwell charge $Q\,(>0)$. Hence, one has also to consider the $\tilde{t} < 0$ region in the coordinates (2.11). In addition, we find that the $\tilde{r} = 0$ surface is neither singular, thereby we may extend the spacetime across the $\tilde{r} = 0$ surface to $\tilde{r} < 0$. Since the allowed region is where $H_T H_S^3 > 0$ is satisfied, we shall focus attention to the coordinate domain

$$\tilde{t} \geq \tilde{t}_s(\tilde{r}), \qquad \tilde{r} \geq -1, \tag{4.6}$$

in the subsequent analysis. Another permitted region $\tilde{t} > \tilde{t}_s$ and $\tilde{r} < -1$ is not our immediate interest here, since it turns out to be causally disconnected to the outside region, as we shall show below. Possible allowed coordinate ranges are depicted in Fig. 1.

Since our spacetime is spherically symmetric, electromagnetic and gravitational fields do not radiate. Thereby, it is more advantageous to concentrate on their "Coulomb components." For this purpose, let us introduce the Newman-Penrose null tetrads by

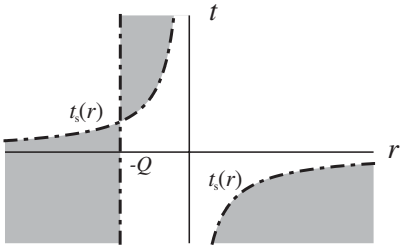

FIG. 1. Allowed coordinate ranges. The gray zones denote the forbidden regions, and the dashed curves correspond to curvature singularities.

$$l_\mu d\tilde{x}^\mu = \sqrt{\frac{\Xi}{2}}(-\tau d\tilde{t} + \Xi^{-1} d\tilde{r}),$$
$$n_\mu d\tilde{x}^\mu = \sqrt{\frac{\Xi}{2}}(-\tau d\tilde{t} - \Xi^{-1} d\tilde{r}), \tag{4.7}$$
$$m_\mu d\tilde{x}^\mu = \frac{\tilde{r}}{\sqrt{2\Xi}}(d\theta + i \sin\theta d\phi),$$

with $\bar{m}_\mu$ being a complex conjugate of m_μ. They satisfy the orthogonality conditions $l^\mu n_\mu = -1 = -m^\mu \bar{m}_\mu$ and $l^\mu l_\mu = n^\mu n_\mu = m^\mu m_\mu = \bar{m}^\mu \bar{m}_\mu = 0$. Since $\tilde{t}$ is a timelike coordinate everywhere, l^μ and n^μ are both future-directed null vectors orthogonal to metric spheres.

The only nonvanishing Maxwell and Weyl scalars are their "Coulomb parts," $\phi_1^{(A)} := -\frac{1}{2} F^{(A)}_{\mu\nu}(l^\mu n^\nu + \bar{m}^\mu m^\nu)$ and $\Psi_2 := -C_{\mu\nu\rho\sigma} l^\mu m^\nu \bar{m}^\rho n^\sigma$, both of which are invariant under the tetrad transformations due to the type D character. It is readily found that

$$\phi_1^{(T)} = \frac{\sqrt{\pi}}{\sqrt{2}\kappa Q \tilde{r}^2 H_T^2}, \qquad \phi_1^{(S)} = \frac{\sqrt{\pi}}{\sqrt{2}\kappa Q \tilde{r}^2 H_S^2}, \tag{4.8}$$

and

$$\Psi_2 = \frac{\Xi_{,\tilde{r}} - \tilde{r}\Xi_{,\tilde{r}\tilde{r}}}{6Q^2\tilde{r}} = \frac{6\tilde{r}H_T^2 + (H_T - H_S)^2 + 2\tilde{t}\,\tilde{r}\,H_S^2}{8Q^2\tilde{r}^4(H_T^5 H_S^7)^{1/2}}. \tag{4.9}$$

The loci of singularities at which these quantities diverge are the same as the positions of the above singularities. One may also recognize that at the fiducial time $\tilde{t} = 1$, the above curvature invariants are the same as the extremal RN solution, as expected.

Let us next look into the causal structure of singularities. Since the Misner-Sharp mass (3.23) becomes negative approaching these singularities [the third term in Eq. (3.23) begins to give a dominant contribution], we speculate from our rule of thumb that these singularities are both contained in the untrapped region and possess the timelike structure.

To see this more rigorously, let us consider radial null geodesics

$$\left.\frac{d\tilde{r}}{d\tilde{t}}\right|_\pm = \pm\tau\tilde{\Xi}, \tag{4.10}$$

in the neighborhood of these singularities. Here, the upper (lower) sign corresponds to the geodesics along the direction l^μ (n^ν), which we shall refer to as outgoing (ingoing). If we can find an infinite number of null geodesics that emanate from and terminate into the singularity, the singularity turns out to be timelike. If there exists a unique geodesic terminating into (emanating from) the singularity and an infinite number of geodesics emanating from (terminating into) it, the singularity has an ingoing (outgoing) null structure. Whereas, if there exist an infinite number of ingoing and outgoing geodesics terminating into or emanating from the singularity, we can conclude that it is spacelike.

We begin by the analysis of the singularity at $\tilde{r} = -1$. In the vicinity of the singularity $\tilde{r} = -1$, we suppose that the null geodesics have the following asymptotic solution:

$$\tilde{r} + 1 = C_1|\tilde{t} - \tilde{t}_1|^p, \tag{4.11}$$

where C_1, $\tilde{t}_1$, and p are constants. C_1 is taken to be positive since we are concerned with the region $\tilde{r} > -1$. $\tilde{t}_1$ can be regarded as the arrival time of the ingoing null geodesics at the singularity, or the departure time of the outgoing null geodesics from the singularity. Consider first the $\tilde{t} > \tilde{t}_1$ case, that is, the geodesics emanating from the singularity. Substituting the assumed form (4.11) into Eq. (4.10), we find that only the outgoing null geodesics have the solution, for which

$$p = \tfrac{2}{5}, \qquad C_1^{5/2} = \tfrac{5}{2}\tau(1 - \tilde{t}_1)^{-1/2}. \tag{4.12}$$

This reveals that for $\tilde{t} > \tilde{t}_1$ there exist radial null geodesics that departed the singularity at $\tilde{t} = \tilde{t}_1$. Following the identical procedure, it can be shown that for $\tilde{t} < \tilde{t}_1$ only the ingoing null geodesics have the solution for which C_1 and p are given by (4.12). This means that there exist radial null geodesics that will get to the singularity at $\tilde{t} = \tilde{t}_1$. Therefore, we establish that the singularity $\tilde{r} = -1$ is truly timelike, that is, a locally naked singularity, since we have only one set of outgoing and ingoing null solutions parametrized by their arrival or emanating time. It is also obvious from Eq. (4.12) that the singularity $\tilde{r} = -1$ exists only for $\tilde{t} < 1$.

In an analogous fashion, assume the asymptotic form of the null geodesics near the singularity $\tilde{r} = \tilde{r}_s (= -1/\tilde{t})$ as

$$\tilde{r} + \frac{1}{\tilde{t}} = C_2|\tilde{t} - \tilde{t}_2|^q, \tag{4.13}$$

where C_2, $\tilde{t}_2$, and q are constants. In the present case, C_2 takes positive (negative) value for $\tilde{t}_2 > 1 (\tilde{t}_2 < 1)$. Plugging this into Eq. (4.10), we obtain $q = 2/3$ and

$$C_2^{3/2} = \tfrac{3}{2}\tau[\tilde{t}_2^2(\tilde{t}_2 - 1)^3]^{-1/2}, \quad \text{for outgoing null with } \tilde{t} > \tilde{t}_2, \tag{4.14a}$$
$$(-C_2)^{3/2} = \tfrac{3}{2}\tau[\tilde{t}_2^2(1 - \tilde{t}_2)^3]^{-1/2}, \quad \text{for ingoing null with } \tilde{t} > \tilde{t}_2, \tag{4.14b}$$
$$C_2^{3/2} = \tfrac{3}{2}\tau[\tilde{t}_2^2(\tilde{t}_2 - 1)^3]^{-1/2}, \quad \text{for ingoing null with } \tilde{t} < \tilde{t}_2, \tag{4.14c}$$
$$(-C_2)^{3/2} = \tfrac{3}{2}\tau[\tilde{t}_2^2(1 - \tilde{t}_2)^3]^{-1/2}, \quad \text{for outgoing null with } \tilde{t} < \tilde{t}_2. \tag{4.14d}$$

Equations (4.14b) and (4.14d) indicate that there exist null geodesics that originate from and come to the singularity at any time $\tilde{t}_2 < 0$. Thus, the singularity $\tilde{t} = -1/\tilde{r} (< 0)$ appearing in the $\tilde{r} > 0$ region is also timelike. Whereas,

Eqs. (4.14a) and (4.14c) show that the timelike singularity $\tilde{r} = -1/\tilde{t}(<0)$ occurs only for $\tilde{t} > 1$.

Although we have not dwelt on the existence proof of the asymptotic solutions [Eqs. (4.11) with (4.12) and (4.13) with (14)] of the radial null geodesics, the proof can be obtained via the contraction mapping method following the argument in e.g., the appendix of [46]. It is also noted that it is sufficient to focus attention on the radial null geodesics in the vicinity of central singularities: causal geodesics excluding radial null geodesics will fail to emanate from singularity if radial null geodesics do not arise (see also the appendix in [46]).

B. Trapping horizons

Our primary concern in this article is to reveal that the spacetime describes a black hole. However, this is not only technically but also conceptually difficult. Since a black hole is by definition a region of no escape, the locus of event horizon as its boundary has a teleological meaning. Unless we know the entire future of our universe, we are unable to determine whether a "black-hole candidate" is qualified as a black hole. The concept of the black hole is considerably messy from a practical point of view.

In physically acceptable situations, however, we can rely on the notion of a *trapped surface*, first introduced by Penrose [47]. The concept of a trapped surface is inherently local; such a difficulty does not arise. Imagine a massive star undergoing a gravitational collapse to form a black hole. There appears a region for which even "outgoing" null rays are dragged back due to strong gravity and have a negative expansion. For each time slice, this defines an *apparent horizon* [22] as an outermost boundary of the trapped region in the asymptotically flat spacetimes. Hayward generalized these quasilocal concepts to define a class of *trapping horizons* [48]. One strength of the use of trapping horizons is just to encompass various types of horizons associated not only with black holes but also with white holes and cosmological ones. As commented at the beginning of this section, the underlying aim of this direction is to gain a useful guide for the event horizon from this local analysis.

Let us consider a compact spacelike orientable surface S. We take S as a metric sphere, respecting an SO(3) symmetry of background universe. It then follows that the Newman-Penrose tetrads (l^μ, n^μ) defined in Eq. (4.7) are normal to S (i.e., they are radial) and future-directed null vectors. Because of the spherical symmetry, they are shear free and rotation free. Define the associated null expansions $\theta_\pm$ by

$$\theta_+ := 2m^{(\mu}\bar{m}^{\nu)}\nabla_\mu l_\nu, \qquad \theta_- := 2m^{(\mu}\bar{m}^{\nu)}\nabla_\mu n_\nu. \quad (4.15)$$

In the coordinates (4.1), they are expressed as

$$\tilde{\theta}_\pm = \frac{\tilde{r}H_S(H_T H_S^3)^{1/2} \pm \tau(3H_T + H_S\tilde{t})}{2\sqrt{2}\tau\tilde{r}(H_T^5 H_S^7)^{1/4}}. \quad (4.16)$$

Note that the signs of $\theta_\pm$ have an invariant meaning, but each value of $\theta_\pm$ is not a universal quantity due to the "class III" tetrad rotations. An invariant combination is their product $\theta_+\theta_- = -2R^{-2}(\nabla_\mu R)(\nabla^\mu R)$.

Expansions $\theta_\pm$ characterize the extent to which the light rays are diverging or converging, or equivalently the rate at which the area of the metric sphere is increasing or decreasing in the null directions. In terms of null expansions $\theta_\pm$, a metric sphere is said to be *trapped* (*untrapped*) if $\theta_+\theta_- > 0$ ($\theta_+\theta_- < 0$), and *marginal* when $\theta_+\theta_- = 0$. A marginal surface is said to be *future* (*past*) if $\theta_+ = 0$ ($\theta_- = 0$). A future marginal surface is further classified into *outer* (*inner*) if $n^\mu\nabla_\mu\theta_+ < 0$ ($n^\mu\nabla_\mu\theta_+ > 0$) and similarly a past marginal surface is called *outer* (*inner*) if $l^\mu\nabla_\mu\theta_- > 0$ ($l^\mu\nabla_\mu\theta_- < 0$). A trapping horizon is the closure of a hypersurface foliated by future or past, and outer or inner marginal surfaces [48]. In terms of the Misner-Sharp energy, $R < 2Gm$ ($R > 2Gm$) defines the trapped (untrapped) region and the marginal surface ($\theta_+\theta_- = 0$) is positioned at the "Schwarzschild radius" $R = 2Gm$. A "normal" spacetime region as occurred in the flat space is composed of untrapped surfaces on which outgoing rays have positive expansions while the ingoing rays have negative expansions.

Among these classes of trapping horizons, the future-outer trapping horizons turn out to be most relevant in the context of black holes. The future-outer trapping horizon properly captures the intuitive idea that the ingoing null rays are converging with the outgoing null ray being instantaneously parallel on the horizon, diverging outside and converging inside. Inner trapping horizons are associated with cosmological horizons, and interior horizons of black holes. The past trapping horizons arise when discussing white holes and cosmological ones. Since the concept of trapping horizons is sufficiently general, it is considerably useful for the analysis of black holes especially in the nonasymptotically flat spacetimes.

The expansions are intimately associated with the variation of the Misner-Sharp energy through the first law [42],

$$\begin{aligned} l^\mu\nabla_\mu m &= 2\pi R^3(T_{\mu\nu}l^\mu n^\nu\theta_+ - T_{\mu\nu}l^\mu l^\nu\theta_-), \\ n^\mu\nabla_\mu m &= 2\pi R^3(T_{\mu\nu}l^\mu n^\nu\theta_- - T_{\mu\nu}n^\mu n^\nu\theta_+). \end{aligned} \quad (4.17)$$

The present system satisfies the dominant energy condition, which implies $T_{\mu\nu}l^\mu l^\nu \geq 0$, $T_{\mu\nu}n^\mu n^\nu \geq 0$, and $T_{\mu\nu}l^\mu n^\nu \geq 0$. Hence, Eq. (4.17) establishes that m is not decreasing (not increasing) along the l^μ direction (n^μ direction) in the untrapped region of $\theta_+ > 0$ and $\theta_- < 0$. This illustrates that the Misner-Sharp energy is a monotonically increasing function toward being outward in the ordinary region where $\theta_+ > 0$ and $\theta_- < 0$ are satisfied, which is in accord with our intuition.

Let us now investigate the properties of trapping horizons more closely. From Eq. (4.16), trapping horizons occur at

$$\tilde{r}H_S(H_T H_S^3)^{1/2} \pm \tau(3H_T + H_S\tilde{t}) = 0, \tag{4.18}$$

where the upper (lower) sign corresponds to $\tilde{\theta}_+ = 0$ ($\tilde{\theta}_- = 0$). Noticing that $\tilde{r}H_S \geq 0$, Eq. (4.18) is solved as $\tilde{t} = \tilde{t}_{\rm TH}^{(\mp)}(\tilde{r})$, where

$$\tilde{t}_{\rm TH}^{(\mp)}(\tilde{r}) := \frac{\tilde{r}^2}{2\tau^2(H_S+3)^2}[H_S^5 - 6\tau^2(H_S+3)\tilde{r}^{-3} \mp H_S^3\sqrt{H_S^4 + 4\tau^2(H_S+3)\tilde{r}^{-3}}]. \tag{4.19}$$

Here, $\tilde{\theta}_\pm = 0$ holds at $\tilde{t} = \tilde{t}_{\rm TH}^{(\mp)}(\tilde{r})$. In the pursuing section, we shall separately analyze the $\tilde{r} > 0$ and $\tilde{r} < 0$ cases corresponding to outside and inside the black-hole event horizon.

Before going into the detailed argument, we pause for a moment to discuss the behavior of $\tilde{R}(\tilde{t}, \tilde{r})$. We have taken l^μ (and correspondingly n^μ) in such a way that $\tilde{r}$ increases (decreases) along $l^\mu(n^\mu)$. From

$$\tilde{R}_{,\tilde{t}} = \frac{|\tilde{r}|}{4}\left(\frac{H_S^3}{H_T^3}\right)^{1/4}, \qquad \tilde{R}_{,\tilde{r}} = \frac{|\tilde{r}|[3H_T + H_S\tilde{t}]}{4\tilde{r}(H_T^3 H_S)^{1/4}}, \tag{4.20}$$

one finds that $\tilde{R}_{,\tilde{r}} > 0$ ($\tilde{R}_{,\tilde{r}} < 0$) holds for $\tilde{t} > \tilde{t}_c(\tilde{r})$ ($\tilde{t} < \tilde{t}_c(\tilde{r})$), where

$$\tilde{t}_c(\tilde{r}) := -\frac{3}{4\tilde{r}+1}. \tag{4.21}$$

This means that $\tilde{R}$ increases as $\tilde{r}$ grows for $\tilde{t} > \tilde{t}_c$, deserving l^μ to be called outgoing. However, this is no longer true for $\tilde{t} < \tilde{t}_c(\tilde{r})$. This means that there exists a maximum value of $\tilde{R}(\tilde{t}, \tilde{r})$ for a given time (see Fig. 2). It should be also remarked that the invariant scalar curvatures are all finite at this surface $\tilde{t} = \tilde{t}_c(\tilde{r})$; this is not the shell-crossing singularity.

1. Trapping horizons in the region of $\tilde{r} > 0$

Let us begin with the case of $\tilde{r} > 0$. After simple calculations, one obtains

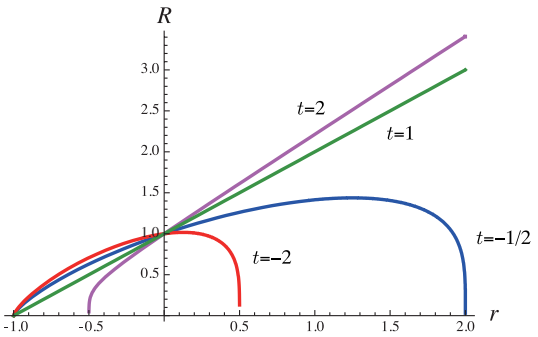

FIG. 2 (color online). Typical behaviors of $\tilde{R} = [(\tilde{t}\,\tilde{r}+1)(\tilde{r}+1)^3]^{1/4}$ as a function of $\tilde{r}$ with fixed time. For fixed $\tilde{t} < 0$, the circumference radius $\tilde{R}$ ceases to increase monotonically with $\tilde{r}$, but has a maximum at $\tilde{t} = \tilde{t}_c(\tilde{r})$. For $\tilde{t} > 0$, $\tilde{R}$ turns to be monotonic in $\tilde{r}$.

$$\tilde{t}_{\rm TH}^{(+)} - \tilde{t}_c(\tilde{r}) = \frac{\tilde{r}^2}{2\tau(H_S+3)^2}(H_S^3\sqrt{H_S^4 + 4\tau^2\tilde{r}^{-3}(H_S+3)} + H_S^5) > 0, \tag{4.22}$$

$$\tilde{t}_c(\tilde{r}) - \tilde{t}_{\rm TH}^{(-)} = \frac{r^2}{2\tau(H_S+3)^2}(H_S^3\sqrt{H_S^4 + 4\tau^2\tilde{r}^{-3}(H_S+3)} - H_S^5) > 0, \tag{4.23}$$

$$\tilde{t}_{\rm TH}^{(-)} - \tilde{t}_s(\tilde{r}) = \frac{\tilde{r}^2}{2\tau(H_S+3)^2}\left[\frac{1}{2}H_S(H_S^2 - \sqrt{H_S^4 + 4\tau^2\tilde{r}^{-3}(H_S+3)})^2 + \frac{1}{2}H_S^5 + \frac{\tau^2}{\tilde{r}^2}H_S(H_S+3)\right] > 0, \tag{4.24}$$

for $\tilde{r} > 0$. Figure 3 shows the typical curves of trapping horizons $\tilde{t}_{\rm TH}^{(\pm)}$. The region $\tilde{t}_{\rm TH}^{(-)} < \tilde{t} < \tilde{t}_{\rm TH}^{(+)}$ denotes a past trapped region in which even ingoing light rays are diverging due to the cosmic expansion.

Next, let us delve deeper into the type of trapping horizon. It is straightforward to find that

$$l^\mu\tilde{\nabla}_\mu\tilde{\theta}_- = \frac{F}{4\tilde{r}^4(H_T^5 H_S^7)^{1/2}}\Big|_{\tilde{t}=\tilde{t}_{\rm TH}^{(+)}}, \tag{4.25}$$

along the trapping horizon with $\tilde{\theta}_- = 0$. Here, we have introduced a function

$$F := H_S^2 - (4\tilde{r}^2 + 8\tilde{r} + 1)H_T^2, \tag{4.26}$$

the sign of which controls the type of trapping horizon. For $\tilde{r} > 0$, the inequality $\tilde{r} + 1 < \sqrt{4\tilde{r}^2 + 8\tilde{r} + 1}$ holds, from

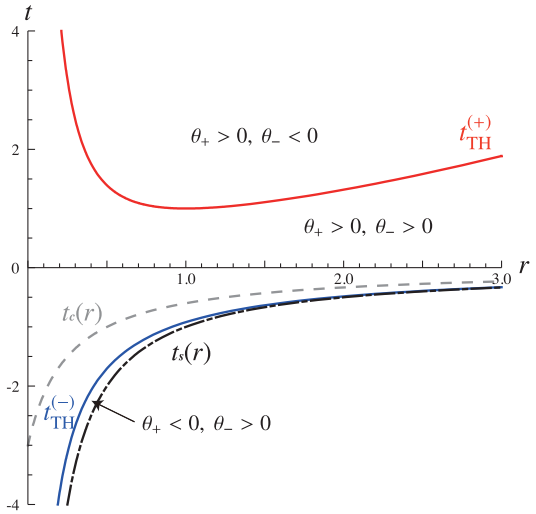

FIG. 3 (color online). Typical curves of trapping horizons $\tilde{t}_{\rm TH}^{(\pm)}(\tilde{r})$ for $\tau < \tau_{\rm crit}$ outside the event horizon $\tilde{r} > 0$. The plot is $\tau = 1$. $\tilde{t}_{\rm TH}^{(+)}$ first occurs at some time (in this case $\tilde{t} = \tilde{r} = 1$) and bifurcates into two branches. The black dashed line and the gray dotted line denote $\tilde{t}_s(\tilde{r})$ and $\tilde{t}_c(\tilde{r})$, respectively.

which we obtain

$$F < -\tilde{t}(H_T + 1/r)(4\tilde{r}^2 + 8\tilde{r} + 1) < 0. \tag{4.27}$$

Hence, for the trapping horizon with $\tilde{t}^{(+)}_{\rm TH} > 0$, $l^\mu \tilde{\nabla}_\mu \tilde{\theta}_- < 0$ is satisfied. That is to say, the past trapping horizon $\tilde{t}^{(+)}_{\rm TH}$ occurring in the $\tilde{r} > 0$, $\tilde{t} > 0$ region is always of an outer type. This may be ascribed to the cosmological origin since a past-outer trapping horizon develops when the background FLRW universe is filled with a stiff matter. A more stringent bound for the condition $F > 0$ is numerically found to be $\tau < \tau_{\rm crit} \sim 5.444$. In the case of $\tau > \tau_{\rm crit}$, a part of the past trapping horizon near $\tilde{r} = 0$ becomes inner rather than outer.

Similarly, we obtain

$$n^\mu \tilde{\nabla}_\mu \tilde{\theta}_+ = \frac{F}{4\tilde{r}^4 (H_T^5 H_S^7)^{1/2}} \Bigg|_{\tilde{t}=\tilde{t}^{(-)}_{\rm TH}}, \tag{4.28}$$

along the trapping horizon with $\tilde{\theta}_+ = 0$. From Eq. (4.23), we find

$$\begin{aligned} F|_{\tilde{t}=\tilde{t}^{(-)}_{\rm TH}(\tilde{r})} &> H_S^2 - (4\tilde{r}^2 + 8\tilde{r} + 1) H_T^2|_{\tilde{t}=\tilde{t}_c} \\ &= 12 H_S^2 (3 + H_S)^{-2} > 0. \end{aligned} \tag{4.29}$$

Hence, the trapping horizon $\tilde{t}^{(-)}_{\rm TH}$ is necessarily of a future-inner type. The appearance of untrapped regions $\tilde{\theta}_+ < 0$ and $\tilde{\theta}_- > 0$ is due to the repulsive nature of the timelike naked singularity.

From the general argument, the outer (inner) trapping horizons must be nontimelike (nonspacelike) under the null energy condition [42,46]. So the above analysis asserts that the trapping horizon $\tilde{t}^{(+)}_{\rm TH}$ never becomes timelike for $\tau < \tau_{\rm crit}$, while $\tilde{t}^{(-)}_{\rm TH}$ cannot be spacelike anywhere.

Here, it is worthwhile to remark the behavior of trapping horizons in various asymptotic limits. In the $\tilde{r} \to 0$ limit, Eq. (4.19) yields that $\tilde{r}\tilde{t}^{(\pm)}_{\rm TH}$ is finite and given by

$$\tilde{r}\tilde{t}^{(+)}_{\rm TH} = \frac{1 + \sqrt{1 + 4\tau^2}}{2\tau^2} > 0, \tag{4.30}$$

$$\tilde{r}\tilde{t}^{(-)}_{\rm TH} = \frac{1 - \sqrt{1 + 4\tau^2}}{2\tau^2} < 0, \tag{4.31}$$

as $\tilde{r} \to 0$. Using this equation, one can find that the circumference radii of the trapping horizons $\tilde{t}^{(\pm)}_{\rm TH}$ respectively approach to some constants $\tilde{R}_\pm$ as $\tilde{r} \to 0$, where

$$\tilde{R}_\pm := \left(\frac{\sqrt{1 + 4\tau^2} \pm 1}{2\tau} \right)^{1/2}. \tag{4.32}$$

These surfaces correspond to the infinite redshift ($\tilde{t} \to \infty$) and blueshift ($\tilde{t} \to -\infty$) surfaces with respect to an asymptotic observer. We will see in the next section that these surfaces represent the black-hole and white-hole horizons. Notice that $\tilde{R}_+$ (and respectively $\tilde{R}_-$) is a monotonically decreasing (increasing) function of τ and they behave as $\tilde{R}_+ \to \infty$ and $\tilde{R}_- \to 0$ in the limit $\tau \to 0$, while they asymptotically tend to unity as $\tau \to \infty$. According to Eq. (4.32), Q and τ are expressed in terms of $R_\pm$ as

$$Q = \sqrt{R_+ R_-}, \qquad \tau = \frac{R_+ R_-}{R_+^2 - R_-^2}. \tag{4.33}$$

Hence, we find that the charge Q sets the geometrical mean of the horizon radii and their relative ratio is encoded in the parameter τ.

The physical meaning of τ is found by evaluating the energy densities of the dilaton field and U(1) field at the horizon R_+ as follows: Those densities are given by

$$\kappa^2 \rho^{(\Phi)}|_{R_+} = \frac{3}{8 t_0^2 \tilde{R}_+^6}, \tag{4.34}$$

$$\kappa^2 \rho^{(\rm em)}|_{R_+} = \frac{1 + 3\tilde{R}_+^8}{4Q^2 \tilde{R}_+^{10}}. \tag{4.35}$$

Then, the ratio is found to be

$$\frac{\rho^{(\rm em)}}{\rho^{(\Phi)}} \Bigg|_{R_+} = \frac{2\tau^2 (1 + 3\tilde{R}_+^8)}{3\tilde{R}_+^4}. \tag{4.36}$$

From the expression of R_+, we find that τ has a one-to-one correspondence to $\rho^{(\rm em)}/\rho^{(\Phi)}|_{R_+}$ and is given by

$$\begin{aligned} \tau^2 &= \frac{1}{8}\left[3\left(\frac{\rho^{(\rm em)}}{\rho^{(\Phi)}} \Bigg|_{R_+} - 1 \right) - \sqrt{3\left(2\frac{\rho^{(\rm em)}}{\rho^{(\Phi)}} \Bigg|_{R_+} - 1 \right)} \right], \\ &\approx \begin{cases} \frac{3}{8} \frac{\rho^{(\rm em)}}{\rho^{(\Phi)}}|_{R_+} & \text{for } \frac{\rho^{(\rm em)}}{\rho^{(\Phi)}}|_{R_+} \gg 2, \\ \frac{1}{4}\left(\frac{\rho^{(\rm em)}}{\rho^{(\Phi)}}|_{R_+} - 2 \right) & \text{for } \frac{\rho^{(\rm em)}}{\rho^{(\Phi)}}|_{R_+} \sim 2. \end{cases} \end{aligned} \tag{4.37}$$

τ is a monotonic function of the ratio, and it vanishes when the ratio approaches 2. The ratio $(\rho^{(\rm em)}/\rho^{(\Phi)})|_{R_+}$, which must be larger than 2 for $\tau^2 > 0$, corresponds to τ by a one-to-one mapping. Hence τ is related to the ratio of two densities at the horizon.

In the limit $\tilde{r} \to 0$, one finds that $\tilde{\theta}_+$ and $\tilde{\theta}_-$ both vanish, implying that the $\tilde{r} = 0$ surface becomes degenerate into an ingoing and outgoing null structure.

On the other hand, taking $\tilde{r} \to \infty$, $\tilde{t}^{(+)}_{\rm TH}$ diverges as $(\tilde{r}^2/4\tau)^2$, whence $\tilde{R}(\tilde{t}^{(+)}_{\rm TH}(\tilde{r}), \tilde{r}) \to \tilde{r}^3/4\tau \to \infty$, while we have $\tilde{t}^{(-)}_{\rm TH} \to -1/\tilde{r} = \tilde{t}_s(\tilde{r})$ as $\tilde{r} \to \infty$. But this does not mean that the trapping horizon $\tilde{t}^{(-)}_{\rm TH}$ plunges into the singularity $\tilde{t}_s$ as $\tilde{r} \to \infty$. One can verify by taking higher order terms into account that $\tilde{t}^{(-)}_{\rm TH}$ tends to have a constant radius $\tilde{R}(\tilde{t}^{(-)}_{\rm TH}(\tilde{r}), \tilde{r}) \to \sqrt{\tau}$ in this limit.

2. Trapping horizons in the region of $r < 0$

For negative values of $\tilde{r}$, $\tilde{t}^{(-)}_{\rm TH} > \tilde{t}^{(+)}_{\rm TH}$ holds, in contrast to the $\tilde{r} > 0$ case. Two trapping horizons $\tilde{t}^{(\pm)}_{\rm TH}$ develop only in the region $\tilde{r}_0 < \tilde{r} < 0$ and they coincide at the point $\tilde{r} = \tilde{r}_0$,

where the square root of Eq. (4.19) vanishes. Namely, $\tilde{r}_0$ satisfies

$$I(\tilde{r}_0) := H_S^4(\tilde{r}_0) + 4\tau^2(H_S(\tilde{r}_0) + 3)\tilde{r}_0^{-3} = 0. \quad (4.38)$$

Since $I(-1) = -12\tau^2 < 0$ and $I(-1/4) = 81 > 0$, $-1 < \tilde{r}_0 < -1/4$ is concluded. We can also find that the trapping horizon $\tilde{t}_{\rm TH}^{(+)}$ negatively diverges at $\tilde{r} = -1/4$. Figure 4 plots typical curves of trapping horizons occurring in $\tilde{r} < 0$.

Equations (4.25) and (4.28) continue to be true for $\tilde{r} < 0$. We can find numerically that at $\tilde{t}_{\rm TH}^{(+)}(\tilde{r})$, $F < 0$ holds around $\tilde{r} \sim 0$ implying that it is spacelike. The future trapping horizon $\tilde{t}_{\rm TH}^{(-)}(\tilde{r})$ and other portions of past trapping horizons $\tilde{t}_{\rm TH}^{(+)}(\tilde{r})$ become timelike. In the limit $\tilde{r} \to 0$, the trapping horizons $\tilde{t}_{\rm TH}^{(\pm)}(\tilde{r})$ have constant circumference radii $\tilde{R}_\pm$ as outside.

3. Constant R surfaces

The trapping horizons occur at $(\tilde{\nabla}_\mu \tilde{R})(\tilde{\nabla}^\mu \tilde{R}) = 0$, i.e., the surfaces of $\tilde{R} =$ const become null. Then the contours of the circumference radius will help us to recognize the positions of trapping horizons in terms of the circumference radius.

Solving Eq. (3.21) with respect to $\tilde{t}$, we obtain

$$\tilde{t} = \frac{1}{\tilde{r}}\left[\frac{\tilde{R}^4}{(1+\tilde{r})^3} - 1\right]. \quad (4.39)$$

Taking the derivative of this equation with fixing $\tilde{R}$, we find the relation between $d\tilde{t}$ and $d\tilde{r}$. Inserting this to the metric (4.1), the line element of $\tilde{R} =$ const surface is given by

$$d\tilde{s}^2 = -\frac{\tau^2(1+4\tilde{r})^2}{\tilde{r}^2\tilde{R}^2(1+\tilde{r})^8}(\tilde{R}^2 - \tilde{R}_1^2)(\tilde{R}^2 + \tilde{R}_1^2) \times (\tilde{R}^2 - \tilde{R}_2^2)(\tilde{R}^2 + \tilde{R}_2^2)d\tilde{r}^2, \quad (4.40)$$

where

$$\tilde{R}_1^2 = \tilde{R}^2(\tilde{t}_{\rm TH}^{(+)}(\tilde{r}), \tilde{r}) = \frac{(1+\tilde{r})^4}{2\tau|1+4\tilde{r}|}\left[1 + \sqrt{1 + \frac{4\tau^2(1+4\tilde{r})}{(1+\tilde{r})^4}}\right], \quad (4.41)$$

$$\tilde{R}_2^2 = \tilde{R}^2(\tilde{t}_{\rm TH}^{(-)}(\tilde{r}), \tilde{r}) = \frac{(1+\tilde{r})^4}{2\tau(1+4\tilde{r})}\left[-1 + \sqrt{1 + \frac{4\tau^2(1+4\tilde{r})}{(1+\tilde{r})^4}}\right]. \quad (4.42)$$

One finds that $\tilde{R}_1 \to \tilde{R}_+$ and $\tilde{R}_2 \to \tilde{R}_-$ in the limit $\tilde{r} \to 0$, and $\tilde{R}_1^2 \to \infty$ and $\tilde{R}_2^2 \to \tau$ as $\tilde{r} \to \infty$. It is notable that $\tilde{R}_1$ and $\tilde{R}_2$ are not independent but fulfill the constraint

$$\tau = \frac{\tilde{R}_1^2\tilde{R}_2^2}{\tilde{R}_1^2 - \tilde{R}_2^2}. \quad (4.43)$$

From $\tilde{R}_1^2 > \tilde{R}_2^2 > 0 > -\tilde{R}_2^2 > -\tilde{R}_1^2$, we conclude that if $\tilde{R}^2 > \tilde{R}_1^2$ or $\tilde{R}^2 < \tilde{R}_2^2$, the $\tilde{R} =$ const curves are timelike, while they are spacelike when $\tilde{R}_2^2 < \tilde{R}^2 < \tilde{R}_1^2$. In the region where $\tilde{R} =$ const curves are timelike (spacelike), and a metric sphere is untrapped (trapped).

We sketch in Fig. 5 the region where $\tilde{R} =$ const curves are timelike (gray region), and spacelike (white region). As $\tilde{r} \to 0$, we find that $\tilde{R}_\pm$ are null surfaces.

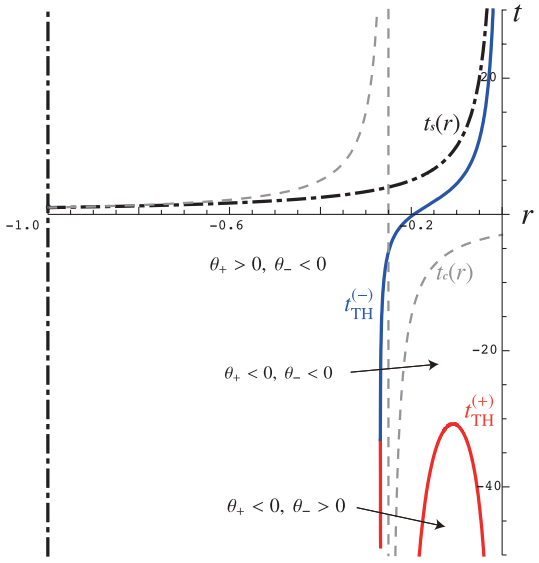

FIG. 4 (color online). Typical curves of trapping horizons $\tilde{t}_{\rm TH}^{(\pm)}(\tilde{r})$ for $\tau < \tau_{\rm crit}$ inside the event horizon $\tilde{r} < 0$. The plot is for $\tau = 1$, for which the trapping horizon $\tilde{t}_{\rm TH}^{(+)}$ has a maximum at $\tilde{r} \simeq -0.1080$, spacelike for $-0.1299 \lesssim \tilde{r} < 0$, and merges with $\tilde{t}_{\rm TH}^{(-)}$ at $\tilde{r}_0 \simeq -0.2679$.

C. Event horizons

Let us proceed to demonstrate the structure of the future- and past-event horizons, utilizing several results obtained in the previous sections.

Before embarking on this program, let us recapitulate the basic features of event horizons. The future-event

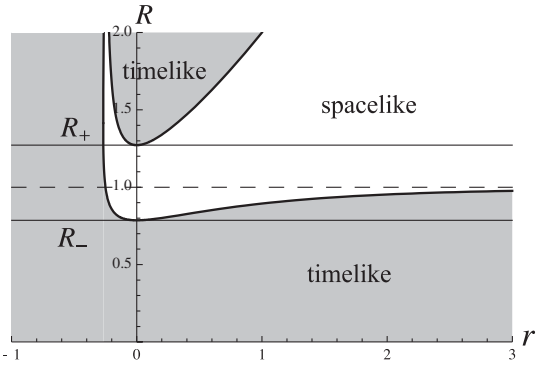

FIG. 5. Signature of $\tilde{R} =$ const surfaces for $\tau = 1$. The $\tilde{R} =$ const curve is timelike (gray regions) and spacelike (white region), which are separated by trapping horizons $\tilde{t}_{\rm TH}^{(\pm)}$.

horizon is defined by a future boundary of the causal past of future null infinity. The past-event horizon is similarly defined by interchanging the role of future and past. These event horizons are by definition the achronal 3D null surfaces. In addition, the future (past) event horizon is generated by null geodesic generators which have no future (past) end point in $(M, g_{\mu\nu})$ [22].

If the spacetime is stationary, the black-hole event horizon must be a Killing horizon [22] (see [49] for the degenerate case). This theorem is considerably significant because it enables us to identify the locus of event horizon simply from the spacetime symmetry. It is *a priori* no interrelationship between the event horizon and the Killing horizon. Such a lucky consequence is exceptional to the stationary case.

In the dynamical case, on the other hand, we have no specific guidelines for identifying the future-event horizon but to evolve the spacetime into the infinite future.[4] Nevertheless, we can say, regardless of this adversity, that the black-hole event horizon has to cover the trapped surfaces, provided the outside region of a black hole is sufficiently well behaved [22]. Inspecting that the spacetime (4.1) appears to have a good behavior at least for $\tilde{r} > 0$ and that the $\tilde{\theta}_{\pm} = 0$ surfaces comprise null surfaces (4.32) in the limit $\tilde{r} \to 0$ and $\tilde{t} \to \pm\infty$, it may be reasonable to consider these null surfaces as the possible candidates of black- and white-hole horizons. Analyzing the near-horizon geometry and behaviors of null geodesics, we shall see below that this expectation is indeed true.

1. Near-horizon geometry

From the behavior of trapped surfaces, we can deduce that the null surface $\tilde{r} = 0$ is a plausible horizon candidate. We shall scrutinize the structure of this surface in detail.

We first look at the throat geometry (2.8). Taking the fiducial time $\tilde{t} = 1$ for simplicity (the same conclusion is derived for any value of finite $\tilde{t}$), the proper distance $\tilde{s}$ from the spacetime point $(1, \tilde{r}, \tilde{\theta}, \tilde{\phi})$ to $(1, \tilde{r} = 0, \tilde{\theta}, \tilde{\phi})$ is given by

$$\tilde{s} = \lim_{\tilde{r}_0 \to 0} \int_{\tilde{r}_0}^{\tilde{r}} \sqrt{\tilde{g}_{\tilde{r}\tilde{r}}(1, \tilde{r})} d\tilde{r} = \lim_{\tilde{r}_0 \to 0} [\tilde{r} + \ln \tilde{r}]_{\tilde{r}_0}^{\tilde{r}} \to \infty. \tag{4.44}$$

This implies that the point $\tilde{r} = 0$ corresponds not to the regular origin of polar coordinates but to "spatial infinity," as in the extremal RN spacetime. In the extremal RN case, the future (past) event horizon is a null surface generated by $\tilde{r} = 0$ and $\tilde{t} = \infty$ $(t = -\infty)$, with its infinite throat at $\tilde{r} = 0$ with $\tilde{t}$ being finite. Analogously, the event horizon of present spacetime, if it exists, should have $\tilde{r} = 0$ with finite $\tilde{t}$ as its throat. So we deduce that the only candidate of event horizons in the present spacetime is $\tilde{r} = 0$ and $\tilde{t} = \pm\infty$.

Therefore, the most convenient way to see the structure of these candidate horizons is to take the *near-horizon limit*, defined by

$$\tilde{t} \to \frac{\tilde{t}}{\epsilon}, \qquad \tilde{r} \to \epsilon \tilde{r}, \qquad \epsilon \to 0, \tag{4.45}$$

where ϵ is a positive constant. Other conceivable limits fail to produce any sensible results. After the rescaling, the coordinate ranges of $\tilde{t}$ and $\tilde{r}$ are free from a restriction other than $\tilde{r} > 0$. Taking the limit (4.45) in Eq. (4.1), one obtains the near-horizon metric:

$$d\tilde{s}^2_{\rm NH} = -\tau^2 \tilde{r}^2 (1 + \tilde{t}\,\tilde{r})^{-1/2} d\tilde{t}^2 + \tilde{r}^{-2} (1 + \tilde{t}\,\tilde{r})^{1/2} (d\tilde{r}^2 + \tilde{r}^2 d\Omega_2^2), \tag{4.46}$$

which does not involve the parameter ϵ. As a direct consequence of (4.45), the near-horizon metric (4.46) is invariant under the flow

$$\xi^\mu = \tilde{t} \left(\frac{\partial}{\partial \tilde{t}} \right)^\mu - \tilde{r} \left(\frac{\partial}{\partial \tilde{r}} \right)^\mu. \tag{4.47}$$

Namely, ξ^μ is a Killing vector in the spacetime (4.46).

Changing the coordinate $\tilde{r}$ to the circumference radius $\tilde{R} = (1 + \tilde{t}\,\tilde{r})^{1/4}$, the near-horizon metric (4.46) transforms into

$$d\tilde{s}^2_{\rm NH} = -f(\tilde{R}) \frac{d\tilde{t}^2}{\tilde{t}^2 \tilde{R}^2} - 8 \frac{\tilde{R}^5}{\tilde{t}(\tilde{R}^4 - 1)} d\tilde{t} d\tilde{R} + \frac{16 \tilde{R}^8}{(\tilde{R}^4 - 1)^2} d\tilde{R}^2 + \tilde{R}^2 d\Omega_2^2, \tag{4.48}$$

where

$$f(\tilde{R}) := \tau^2 (\tilde{R}^4 - 1)^2 - \tilde{R}^4 = \tau^2 (\tilde{R}^4 - \tilde{R}_+^4)(\tilde{R}^4 - \tilde{R}_-^4). \tag{4.49}$$

Here, $\tilde{R}_+$ and $\tilde{R}_-$ have been defined in Eq. (4.32). In the coordinates (4.48), we have $\xi^\mu = \tilde{t}(\partial/\partial \tilde{t})^\mu$. Apart from $\tilde{R} = 0$ (which is indeed a curvature singularity) and the points at $\theta = 0, \pi$ (which are north and south poles of a 2-sphere), there appear additional coordinate singularities at $\tilde{t} = 0$ and $\tilde{R} = 1$ in the metric (4.48).

Although the metric (4.48) is time dependent, we can eliminate the time dependence of the metric (4.48) by changing to the time slice,

$$\eta_\pm := \ln(\pm \tilde{t}), \quad \text{for } \tilde{t} \gtrless 0, \tag{4.50}$$

[4]The Sultana-Dyer solution [34] is an exceptional instance: it is conformal to the Schwarzschild metric, and hence its causal picture is extracted in a simple fashion [50]. It deserves to mention that the values of surface gravities are sensitive to the norm of the generator ξ^μ of the Killing horizon. The spacetime (4.53) is not asymptotically flat; hence there exists no meaningful way to fix the values. (In the asymptotically flat case, we usually require at infinity $\xi_\mu \xi^\mu \to -1$, which eliminates the ambiguity.) However, this ambiguity causes no harm in our present discussion. The important point to note here is that they take nonvanishing positive values. We will revisit this issue when we discuss thermodynamics in the ensuing section.

in terms of which the Killing vector is written as $\xi^\mu = (\partial/\partial\eta_\pm)^\mu$ and the near-horizon metric (4.48) is given by

$$d\tilde{s}^2_{\rm NH} = -\frac{f(\tilde{R})}{\tilde{R}^2}\left[d\eta_\pm + \frac{4\tilde{R}^7}{(\tilde{R}^4-1)f(\tilde{R})}d\tilde{R}\right]^2 + \frac{16\tau^2\tilde{R}^8}{f(\tilde{R})}d\tilde{R}^2 + \tilde{R}^2 d\Omega_2^2. \quad (4.51)$$

The sign of $\eta_\pm$ has been chosen in such a way that $\eta_+(\eta_-)$ increases (decreases) as $\tilde{t}$ increases.

Performing a further coordinate transformation,

$$\tilde{T}_\pm = \eta_\pm + \int^{\tilde{R}} \frac{4\tilde{R}^7}{(\tilde{R}^4-1)f(\tilde{R})}d\tilde{R}, \quad (4.52)$$

the near-horizon metric (4.51) is brought into a familiar form,

$$d\tilde{s}^2_{\rm NH} = -\frac{f(\tilde{R})}{\tilde{R}^2}d\tilde{T}^2_\pm + \frac{16\tau^2\tilde{R}^8}{f(\tilde{R})}d\tilde{R}^2 + \tilde{R}^2 d\Omega_2^2. \quad (4.53)$$

This metric describes a static black hole whose horizons occur where the lapse function vanishes $f(\tilde{R}) = 0$, i.e., where the Killing field $\xi^\mu = (\partial/\partial\tilde{T}_\pm)^\mu$ becomes null. The condition $f(\tilde{R}) = 0$ gives two roots $\tilde{R} = \tilde{R}_\pm$ given by Eq. (4.32), which coincide with the trapping horizons in the $\tilde{r} \to 0$ limit taken. Thus, we conclude that the null surfaces $\tilde{R} = \tilde{R}_\pm$ in the original spacetime are locally isometric to the Killing horizons in the static spacetime (4.53).

Reminding one of the fact that the outside domain of the original spacetime (4.1) is highly dynamical and hence is lacking a nonspacelike Killing field, it comes as a novel surprise for us that the near-horizon metric (4.53) permits the unexpected symmetry (4.47). Observe that the vector field (4.47) satisfies the Killing equation in the original spacetime (4.1) *only at the horizon* $\tilde{R} = \tilde{R}_\pm$. This may be ascribed to the fact that the 11D solution is supersymmetric if all branes are at rest. The supersymmetry does not allow energy inflow, consistent with the property that the Killing horizon is totally geodesic. This may be clear by considering the Raychaudhuri equation: $T_{\mu\nu}\xi^\mu\xi^\nu \to 0$ is indeed satisfied in the limit (4.30) or (4.31). As far as the authors know, this is the first realization of asymptotic symmetry appearance at the black-hole horizon under the dynamical circumstance.

Let us devote some space here to discuss the near-horizon static metric (4.53) in more detail. In this limit, the dilaton (3.8) and the Maxwell fields (3.9) are reduced to

$$\kappa\Phi = \sqrt{6}\ln\tilde{R}, \quad (4.54)$$

and

$$\kappa\tilde{F}^{(T)} = -4\sqrt{2\pi}\tau\tilde{R}^{-5}d\tilde{T}\wedge d\tilde{R}, \qquad \kappa\tilde{F}^{(S)} = -4\sqrt{2\pi}\tau\tilde{R}^{3}d\tilde{T}\wedge d\tilde{R}. \quad (4.55)$$

We can confirm Eqs. (4.53), (4.54), and (4.55) still satisfy the original field equations (3.3), (3.4), and (3.5), which justifies the fact that the near-horizon limit (4.45) is well defined. It is obvious that the near-horizon metric (4.53) describes a static black hole, whose asymptotic structure is neither flat nor AdS. Such an unusual asymptotic structure is, however, that one commonly encountered in Einstein-Maxwell-dilaton gravity (see e.g., [51,52]). Albeit this peculiar asymptotics, it is easy to find that the causal structure is akin to that of the nonextremal RN-AdS solution (see Fig. 6). The spatial infinity $\tilde{R} \to \infty$ consists of a timelike boundary $\mathcal{I}$, a timelike singularity resides at the center $\tilde{R} = 0$, and the two distinct outer and inner horizons $\tilde{R}_\pm$ of black hole and white hole arise.

Since $\tilde{R}_+$ is strictly larger than $\tilde{R}_-$ for finite τ [see Eq. (4.33)], we find that the horizons are not degenerate. From the general formula $\kappa^2_\pm = \mp(1/2)(\nabla_\mu\xi_\nu)\nabla^\mu\xi^\nu$, one obtains the surface gravities of these horizons,

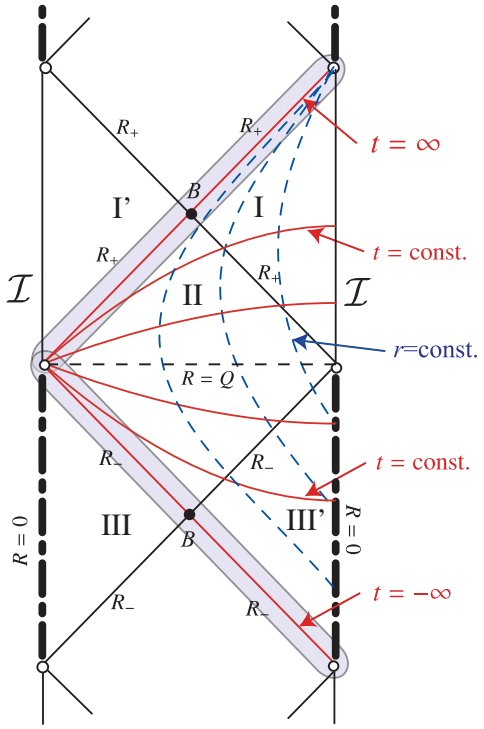

FIG. 6 (color online). Conformal diagram of a maximally extended near-horizon metric (4.53). The black hole has outer and inner horizons, whose radii are, respectively, given by $\tilde{R}_+$ and $\tilde{R}_-$. Infinity consists of a timelike surface denoted by $\mathcal{I}$. The white circles mark points at infinity (i^0, $i^\pm$, or the throat) and should not be regarded as spacetime events. The filled circles B represent bifurcation surfaces *for the metric* (4.53) at which $\xi^\mu = (\partial/\partial T_\pm)^\mu$ vanishes, i.e., B's are the fixed points under this isometry. Thick red lines correspond to $\tilde{t}$ = const surfaces, and blue dotted lines denote $\tilde{r}$ = const surfaces. $\tilde{R} = 1$ is a coordinate singularity for the metric (4.48) corresponding to $\tilde{t} = 0$. The shaded regions approximate our dynamical metric (4.1) in the neighborhood of horizons.

$$\kappa_\pm = \pm \frac{f'(\tilde{R}_\pm)}{8\tau\tilde{R}_\pm^5} = \frac{\sqrt{1+4\tau^2}}{\sqrt{1+4\tau^2}\pm 1}, \tag{4.56}$$

where κ_+ and κ_- are the surface gravity of the outer and inner event horizons, respectively. The surface gravity of the Killing horizon is constant over the horizon, illustrating the equilibrium state. The nonvanishing surface gravity might be seemingly puzzling, in light of the situation that the 11D solution was "maximally charged" because of the supersymmetry in the static limit.

Introduce the null coordinates $u_\pm$ by

$$u_\pm = \tilde{T}_\pm - \int^{\tilde{R}} \frac{4\tau\tilde{R}^5}{f(\tilde{R})} d\tilde{R} = \ln[\pm\tilde{t}|\tilde{R}^4 - 1|^{-1}|\tilde{R}^2 + \tilde{R}_+^2|^{1/\kappa_+}|\tilde{R}^2 - \tilde{R}_-^2|^{1/\kappa_-}], \tag{4.57}$$

where the integration follows from a direct calculation by Eqs. (4.49), (4.52), and (4.56). The coordinates $u_\pm$ are well defined at $\tilde{R} = \tilde{R}_+$. Using $u_\pm$, the metric (4.53) is translated into the single null form,

$$d\tilde{s}^2_{\rm NH} = -\frac{f(\tilde{R})}{\tilde{R}^2} du_\pm^2 - 2du_\pm d\tilde{R} + \tilde{R}^2 d\Omega_2^2. \tag{4.58}$$

Let us consider the plus coordinate in Eq. (4.58) and discuss the outer white-hole horizon (the boundary of I' and II). It is immediate to find that the null generator of the Killing horizon ξ^μ is expressed in these coordinates as $\xi^\mu = (\partial/\partial u_+)^\mu$. u_+ is the Killing parameter ($\xi^\mu\nabla_\mu u_+ = 1$) of null geodesic generators. It then follows that the renormalized tangent vector,

$$k^\mu = \frac{1}{\kappa_+} e^{\kappa_+ u_+} \left(\frac{\partial}{\partial u_+}\right)^\mu, \tag{4.59}$$

is affinely parametrized, i.e., k^μ satisfies the zero-acceleration geodesic equation $k^\nu\nabla_\nu k^\mu = 0$ on the horizon. (Note that we are considering a white hole so that $\xi^\nu\nabla_\nu\xi^\mu = -\kappa_+\xi^\mu$.) This means that the affine parameter λ [$k^\mu = (\partial/\partial\lambda)^\mu$] is related to the Killing parameter u_+ as

$$\lambda = -e^{-\kappa_+ u_+}. \tag{4.60}$$

This manifests the affine parameter λ values from $-\infty$ to 0 as u_+ ranges from $-\infty$ to ∞, implying the bifurcation surface—a closed surface at which ξ^μ vanishes. This can be verified by noticing $\xi^\mu = (\partial/\partial\tilde{T}_+) = \kappa_+\lambda(\partial/\partial\lambda)^\mu \to 0$ as $\lambda \to 0$. A similar argument goes through to u_-. Therefore, the nondegenerate Killing horizon (i.e., a Killing horizon with nonvanishing surface gravity) is incomplete either into the past or future. This is a general consequence of a Killing horizon [21].

However, the above discussion does not mean that the horizon in our original spacetime is the bifurcate Killing horizon. This is consistent with results in [53] which asserts that the nondegenerate Killing horizon is the bifurcate Killing horizon. In their proof, it is assumed that the horizon is smooth (C^∞ class), while the horizon in the present case is only finite times differentiable (C^k class with k finite) (see Sec. IV C 3).

To summarize this section, we can expect that the original spacetime (4.1) would have the future-event horizon at $\tilde{r} \to 0$ with $\tilde{t} \to \infty$, and the past-event horizon at $\tilde{r} \to 0$ with $\tilde{t} \to -\infty$. We have found that the point at $\tilde{r} = 0$ with $\tilde{t}$ being finite corresponds to "throat infinity" just as that of the extreme RN spacetime, at which future- and past-event horizons should intersect. In the neighborhood of these horizon candidates, the spacetime (4.1) is approximated by the near-horizon geometry (4.53) with Killing horizons, in which several portions of Killing horizons with radii $\tilde{R}_\pm$ appear. What portion of Killing horizons in Fig. 6 corresponds to the horizon in our original spacetime? The answer is obvious: the "white-hole portion" (gray-colored line segment encompassing blocks I, II, and III' in Fig. 6) only satisfies the above criteria.

2. Null geodesics

We marked out $\tilde{R}_+$ as a black-hole horizon in the spacetime (4.1). To conclude this more rigorously, we face up the problem of solving geodesic motions. Since the present spacetime is spherically symmetric, it suffices us to focus on radial null geodesics to argue causal structures. Although examinations of nonradial and/or timelike geodesic motions are important issues in order to clarify the detailed physical properties of the solution, we will not discuss these since behaviors of radial null geodesics are sufficient to determine the causal structure.

The radial null geodesic equations are governed by

$$\ddot{\tilde{t}} - \frac{1}{4H_T}\dot{\tilde{t}}^2 + \frac{(H_S+3H_T)}{2\tilde{r}^2H_TH_S}\dot{\tilde{t}}\dot{\tilde{r}} + \frac{H_S^3}{4\tau^2}\dot{\tilde{r}}^2 = 0, \tag{4.61}$$

$$\ddot{\tilde{r}} + \frac{\tau^2(H_S+3H_T)}{4\tilde{r}^2H_T^2H_S^4}\dot{\tilde{t}}^2 + \frac{1}{2H_T}\dot{\tilde{t}}\dot{\tilde{r}} - \frac{(H_S+3H_T)}{4\tilde{r}^2H_TH_S}\dot{\tilde{r}}^2 = 0, \tag{4.62}$$

$$-\tau^2\dot{\tilde{t}}^2 + H_TH_S^3\dot{\tilde{r}}^2 = 0, \tag{4.63}$$

where the dot denotes a differentiation with respect to an affine parameter λ. These equations are combined to give

$$\ddot{\tilde{t}} \pm \frac{\tau(H_S+3H_T)}{2\tilde{r}^2(H_T^3H_S^5)^{1/2}}\dot{\tilde{t}}^2 = 0, \tag{4.64}$$

$$\ddot{\tilde{r}} \pm \frac{(H_TH_S^3)^{1/2}}{2\tau H_T}\dot{\tilde{r}}^2 = 0, \tag{4.65}$$

where the plus (minis) sign refers to the outgoing (ingoing) geodesics. Unfortunately, the radial null geodesics do not appear to admit a first integral other than Eq. (4.63), so it is not amendable to analytic study. Instead, we try to solve numerically Eqs. (4.64) and (4.65) subjected to the initial

constraint (4.63). Making use of the degrees of freedom of the affine parameter $\lambda \to a\lambda + b$, we are able to choose $\lambda = 0$ at the starting point of the geodesics and set $\dot{\tilde{t}}(0)$ at any values we wish. Fixing the orientation of future-directed geodesics to be $\dot{\tilde{t}} > 0$, and past-directed to be $\dot{\tilde{t}} < 0$, we choose $\dot{\tilde{t}}(0) \equiv 1(-1)$ for future- (past-) directed radial null geodesics without loss of generality. Hence the residual freedoms that distinguish different geodesics are two, corresponding to the initial values [$\tilde{t}(0)$ and $\tilde{r}(0)$] for each $\tau > 0$.

Let us begin our consideration by the geodesics in the outside region $\tilde{r} > 0$. Taking the representative spacetime events p_I ($I = 1, 2, 3$) such that $\tilde{t}_1 > \tilde{t}_{\rm TH}^{(+)}$, $\tilde{t}_{\rm TH}^{(-)} < \tilde{t}_2 < \tilde{t}_{\rm TH}^{(+)}$, and $\tilde{t}_3 < \tilde{t}_{\rm TH}^{(-)}$ where $\tilde{t}_I \equiv \tilde{t}|_{p_I}$ (see Fig. 3), we have examined behaviors of geodesics starting from $\tilde{t} = \tilde{t}_I$. We call the geodesics emanating from the event p_I as class I. Since $\tilde{R}_1 > \tilde{R}_+$ ($\tilde{R}_2 < \tilde{R}_-$), class 1 (class 3) geodesics initially have a circumference radius larger (smaller) than $\tilde{R}_+$ ($\tilde{R}_-$).

We depict several typical geodesic curves emanating from ($\tilde{t}_I$, $\tilde{r}(0) = 1$) for $\tau = 1$ in Fig. 7. This is a representative figure for $\tau < \tau_{\rm crit}$. Qualitative behavior of geodesics seems not so sensitive to the initial radial position $\tilde{r}(0)$. The numerical results are summarized as follows:

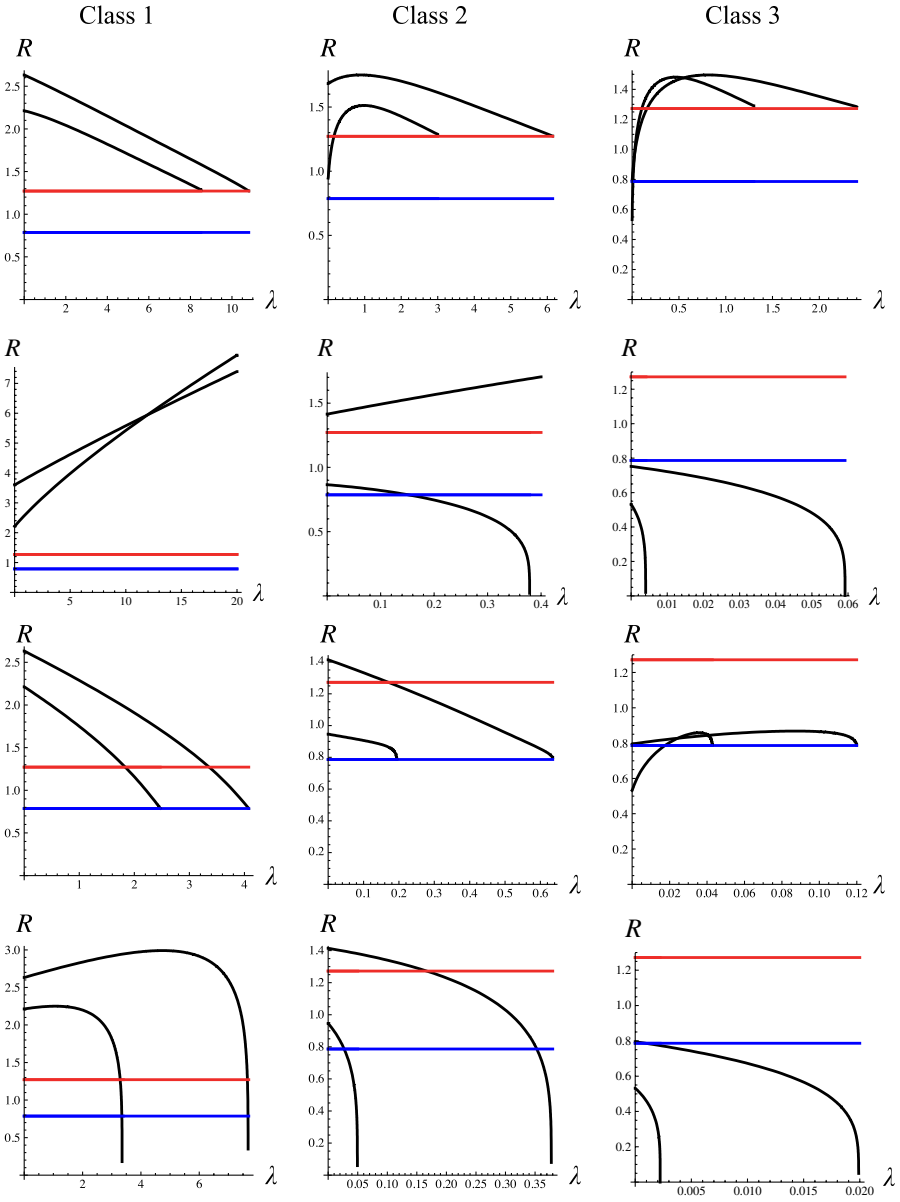

FIG. 7 (color online). Radial null geodesics in the outside region ($\tilde{r} > 0$) emanating from $\tilde{t}(0) = \tilde{t}_I$ and $\tilde{r}(0) = 1$ for $\tau = 1$. The diagrams in the top, upper middle, lower middle, and bottom rows correspond to future-directed ingoing null geodesics, future-directed outgoing null geodesics, past-directed ingoing null geodesics, and past-directed outgoing null geodesics, respectively. The red and blue lines denote $\tilde{R}_+ \sim 1.27$ and $\tilde{R}_- \sim 0.786$, respectively.

(i) *Future-directed ingoing null geodesics:* Class 1 geodesics monotonically decrease the circumference radius and arrive at $\tilde{R}_+$ within a finite affine time. Class 2 geodesics first increase the circumference radius since they are originally in the trapped region $\tilde{\theta}_- > 0$. But they always move across $\tilde{t}_{\rm TH}^{(+)}$, and finally reach $\tilde{R}_+$ with decreasing area. The qualitative behavior of class 3 is the same as that of class 2, except that class 3 geodesics always cross $\tilde{R} = \tilde{R}_+$ twice, and if $\tilde{t}_3$ is sufficiently close to $\tilde{t}_s$, they may cross $\tilde{R}_-$. All classes of geodesics have infinite redshift $\tilde{t}(\lambda) \to +\infty$ when they finally arrive at $\tilde{R}_+$.

(ii) *Future-directed outgoing null geodesics:* Class 1 geodesics necessarily go out to infinity $\tilde{R} \to \infty$. Class 2 geodesics may extend out to infinity or arrive at the singularity $\tilde{t} = \tilde{t}_s$ if $\tilde{t}_2$ is small. Class 3 geodesics inevitably plunge into the singularity $\tilde{t} = \tilde{t}_s$ within a finite affine time.

(iii) *Past-directed ingoing null geodesics:* Class 1 geodesics originate from $\tilde{R} > \tilde{R}_+$ and their radii monotonically decrease toward $\tilde{R}_-$. Class 2 geodesics have qualitatively the same behavior. Class 3 geodesics start from $\tilde{R} < \tilde{R}_-$ with increasing area, then cross $\tilde{R}_-$ (with finite $\dot{\tilde{t}}$), attain the maximum radius, and get back to $\tilde{R}_-$ again with undergoing infinite blueshift.

(iv) *Past-directed outgoing null geodesics:* Class 1 geodesics may initially increase the area, but all geodesics unavoidably terminate into the singularity $\tilde{t} = \tilde{t}_s$ within a finite affine time.

From these results, we conclude that the null surfaces $\tilde{R} = \tilde{R}_\pm$ locate within a finite affine time from outside spacetime events. Behaviors of future-directed outgoing null rays of class 2 geodesics imply that there exists a critical null curve $\tilde{t} = \tilde{t}_*(\tilde{r})$ such that outgoing rays emanating from $\tilde{t} > \tilde{t}_*$ can get to infinity, whereas outgoing rays emanating from $\tilde{t} < \tilde{t}_*$ fall into the singularity.

Let us discuss next the geodesics inside the horizon. We call class 1 as $\tilde{t} > \tilde{t}_1 > \tilde{t}_{\rm TH}^{(-)}$, class 2 as $\tilde{t}_{\rm TH}^{(-)} > \tilde{t}_2 > \tilde{t}_{\rm TH}^{(+)}$, and class 3 as $\tilde{t}_{\rm TH}^{(+)} > \tilde{t}_3$ (see Fig. 4). Figure 8 plots the geodesic curves emanating from the spacetime event $[t_I, \tilde{r}(0) = -1/10]$ with $\dot{\tilde{t}}(0) = \pm 1$. Geodesics starting from $\tilde{r}(0) < \tilde{r}_0$ show the same behavior as class 1. The results are as follows:

(i) *Future-directed ingoing null geodesics:* Class 1 geodesics and class 2 geodesics starting from not so small $\tilde{t}_2$ eventually fall into the singularity $\tilde{t} = \tilde{t}_s$. Class 2 geodesics with $\tilde{t}_2$ close to $\tilde{t}_{\rm TH}^{(+)}(\tilde{r})$ fall into the singularity $\tilde{r} = -1$ within a finite affine time. Class 3 geodesics initially increase area, but they eventually plunge into the singularity at $\tilde{r} = -1$.

(ii) *Future-directed outgoing null geodesics:* Class 1 geodesics increase area and approach $\tilde{R} = \tilde{R}_-$ with infinite redshift $\tilde{t}(\lambda) \to +\infty$. Class 2 and class 3 geodesics decrease area and arrive at $\tilde{R} = \tilde{R}_-$ with infinite redshift $\tilde{t}(\lambda) \to +\infty$.

(iii) *Past-directed ingoing null geodesics:* Class 1 geodesics monotonically reduce area and fall into the singularity $\tilde{t} = \tilde{t}_s$. Class 2 and class 3 geodesics initially grow the area and then turn to decrease, and finally fall into the singularity $\tilde{r} = -1$.

(iv) *Past-directed outgoing null geodesics:* All geodesics eventually approach $\tilde{R} = \tilde{R}_+$ with infinite blueshift $\tilde{t}(\lambda) \to -\infty$.

From these results, the null surface $\tilde{R} = \tilde{R}_-$ has an ingoing null structure, analogous to the white-hole horizon or the black-hole inner horizon.

3. Asymptotic solutions of geodesics

We have numerically established that the radial null geodesics are incomplete at the null surfaces $\tilde{R} = \tilde{R}_\pm$. We shall look into the asymptotic geodesic solutions and discuss further the horizon structure.

If a null geodesic is known as $\tilde{t} = \tilde{t}(\tilde{r})$, the affine parameter λ is obtained by a simple quadrature [38]

$$\lambda = \int d\tilde{r} \exp\left[\pm \int U[\tilde{t}(\tilde{r}'), \tilde{r}'] dr' \right], \tag{4.66}$$

where we have used the shorthand notation

$$U = \frac{(H_T H_S^3)^{1/2}}{2\tau H_T}. \tag{4.67}$$

In the event horizon limit (4.30), we have

$$U \to \frac{1}{\tilde{r}(1 + \sqrt{1 + 4\tau^2})}. \tag{4.68}$$

Substituting this into Eq. (4.66) and solving with respect to the radial coordinate, we obtain the asymptotic solution of the future-directed null geodesic around the horizon $\tilde{R} = \tilde{R}_+$ as

$$\tilde{r} = c_1^{(+)}(\lambda - \lambda_+)^{1/\kappa_+}, \qquad \tilde{t} = c_2^{(+)}(\lambda - \lambda_+)^{-1/\kappa_+}, \tag{4.69}$$

where λ_+ corresponds to the arrival time for the geodesics at the horizon, and $c_1^{(+)}$ and $c_2^{(+)}$ are positive constants satisfying $c_1^{(+)} c_2^{(+)} = (1 + \sqrt{1 + 4\tau^2})/(2\tau^2)$. κ_+ has been given in Eq. (4.56). We can find from Eq. (4.69) that the radial geodesics indeed reach the horizon within a finite affine time [38]. Equation (4.69) implies that $\tilde{r}$ and $\tilde{t}$ are not smooth functions of λ (note that $1/\kappa_+$ never takes an integer).

Similarly, we obtain

$$\tilde{r} = c_1^{(-)}(\lambda - \lambda_-)^{1/\kappa_-}, \qquad \tilde{t} = c_2^{(-)}(\lambda - \lambda_-)^{-1/\kappa_-}, \tag{4.70}$$

for an outgoing null geodesic near the horizon $\tilde{R} = \tilde{R}_-$. Constants $c_1^{(-)}$ and $c_2^{(-)}$ satisfy $c_1^{(-)} c_2^{(-)} = (1 - \sqrt{1 + 4\tau^2})/(2\tau^2)$.

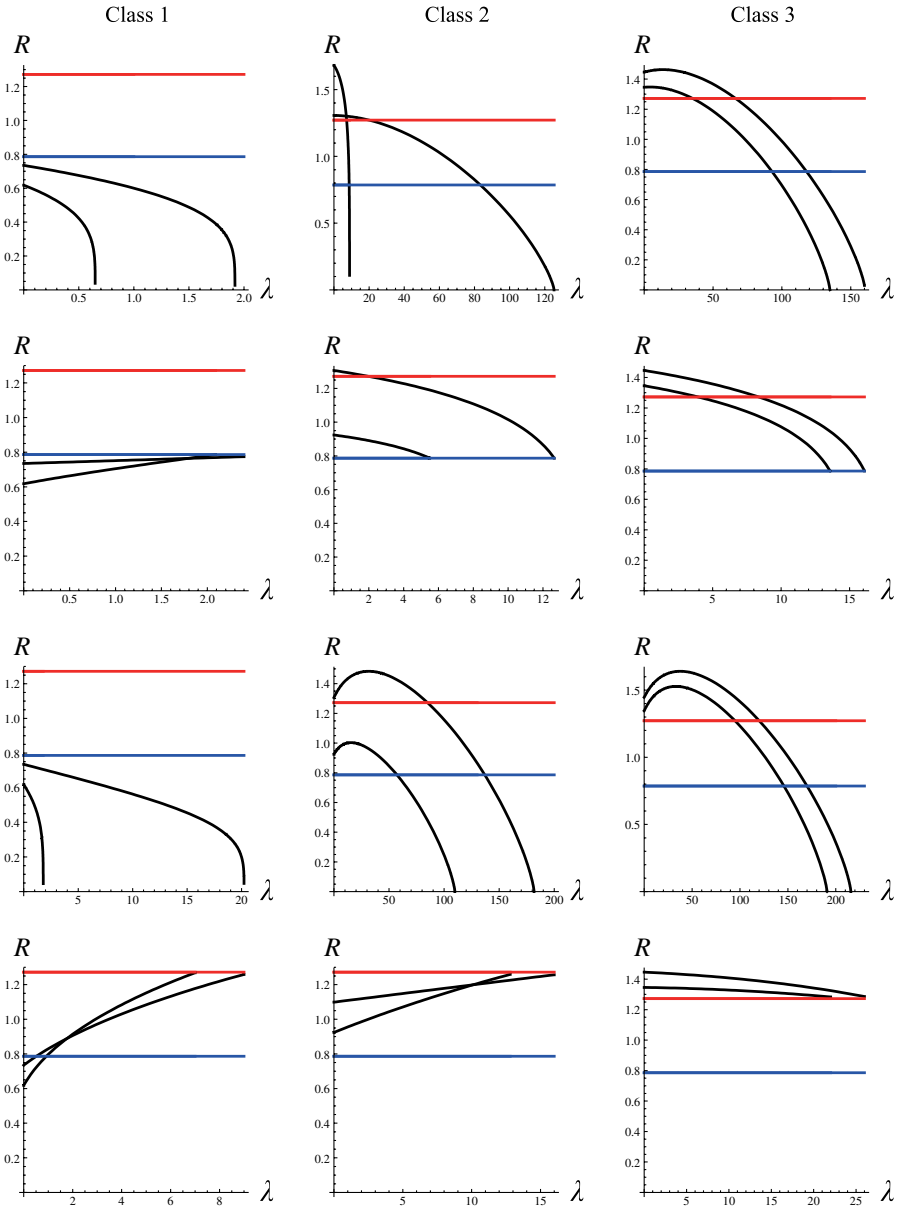

FIG. 8 (color online). Radial null geodesics in the inside region ($\tilde{r} < 0$) emanating from $\tilde{t}(0) = \tilde{t}_I$ and $\tilde{r}(0) = -1/10$ for $\tau = 1$. The diagrams in the top, upper middle, lower middle, and bottom rows correspond to future-directed ingoing null geodesics, future-directed outgoing null geodesics, past-directed ingoing null geodesics, and past-directed outgoing null geodesics. The red and blue lines denote $\tilde{R}_+ \sim 1.27$ and $\tilde{R}_- \sim 0.786$, respectively.

D. Carter-Penrose diagram

We are now in a position to discuss global causal structures of spacetime, by assembling considerations hitherto obtained. The optimal way to appreciate the large scale causal structure is to draw the Carter-Penrose conformal diagram, which enables us to visually capture the global light-cone fabric. We first notice the following:

(i) The only candidates of future- and past-event horizons are $\tilde{r} = 0$ and $\tilde{t} \to \pm\infty$, which are joined at the throat at $\tilde{r} = 0$ and $\tilde{t}$ being finite.

(ii) The near-horizon geometry of the event horizons is locally isometric to that of the static black hole (4.53). The white-hole portion corresponds to the horizon in the original spacetime (2.1) with the bifurcation surface replaced by a smooth surface.

(iii) There are the curvature singularities at $\tilde{t} = \tilde{t}_s(r) = -1/\tilde{r}$ and $\tilde{r} = -1$. These singularities are timelike (Sec. IVA). The time-dependent singularity $\tilde{t}_s(\tilde{r})$ present in the $\tilde{r} < 0$ domain exists for $\tilde{t} > 1$, whereas $\tilde{t}_s(\tilde{r})$ lying in the $\tilde{r} > 0$ region and the other singularity $\tilde{r} = -1$ exist for eternity.

These observations prompt us to imagine the positional relation between singularities and the horizons. Figure 9 describes the conformal diagram of our dynamical black

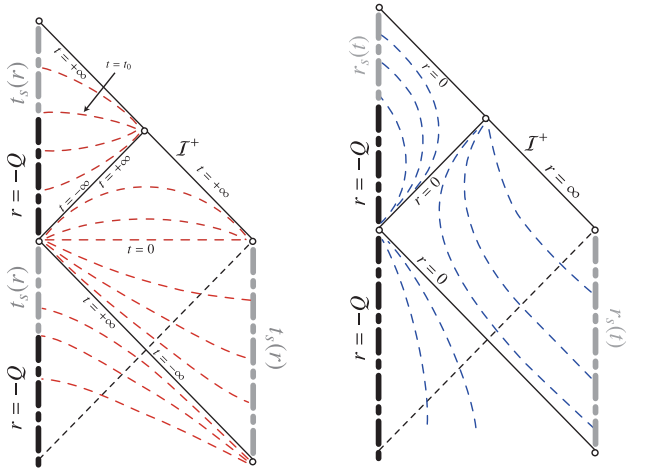

(a) The contour of $\tilde{t}$ = constant. (b) The contour of $\tilde{r}$ = constant.

FIG. 9 (color online). Conformal diagram of the spacetime (4.1). We draw (a) the contour (spacelike) curves of $\tilde{t}$ = const by red lines and (b) the contour (timelike) curves of $\tilde{r}$ = const by blue lines. The singularity of $\tilde{R} = 0$ consists of three parts: a black-hole singularity at $\tilde{r} = -1$ and at $\tilde{r} = \tilde{r}_s(\tilde{t}) = -1/\tilde{t}$ inside the horizon, and a "big-bang singularity" $\tilde{t} = \tilde{t}_s(\tilde{r}) = -1/\tilde{r}$ outside the horizon.

hole. From properties (i) and (ii), we can depict the identical horizon structure as in Fig. 6. Since the $\tilde{t}$ = const ($<\infty$) lines are everywhere spacelike, each slice originates from the throat $\tilde{r} = 0$. For negative values of $\tilde{t}$, $\tilde{t}$ = const surfaces must intersect the singularity $\tilde{t}_s(\tilde{r})$ at finite $\tilde{r}$ (see Fig. 3). Considering property (iii) that the singularity outside the horizon is only $\tilde{t} = \tilde{t}_s(\tilde{r}) < 0$, the right side dotted portion of the gray line can be drawn in Fig. 9. Outside the horizon $\tilde{r} > 0$, one can depict the contours of $\tilde{t}$ = const and $\tilde{r}$ = const family of surfaces, both of them to be orthogonal (Fig. 9). These aspects are all consistent with our numerical survey of geodesics. We thus conclude that the spacetime metric (4.1) indeed describes a black hole in the FLRW universe [aside from the undesirable timelike naked singularity $\tilde{t}_s(\tilde{r})$]. Although the null surface $\tilde{R}_-$ is a one-way membrane of a "region of no entrance," it does not deserve to be a white-hole horizon in a mathematical sense since the spacetime does not possess the past null infinity.

Inside the event horizon $\tilde{R} < \tilde{R}_+$, the timelike singularities are vertically joined at $\tilde{t} = -1$. The past boundary $\tilde{R}_+$ can be matched to the black-hole horizon. We can find as sketched in Fig. 9 that these patches are infinitely arrayed vertically. It should be emphasized, however, that this is only a possible extension, since the horizon is not analytic in the present case. One may glue the near-horizon geometry (4.46) to the spacetime (4.1) across the horizon.

Next, we wish to fill in the trapping horizons into this diagram (we only consider the $\tau = 1$ case). We should remind one of the following remarks:

(i) There are trapping horizons $\tilde{t} = \tilde{t}_{\rm TH}^{(\pm)}$ at which $\tilde{\theta}_\mp = 0$. Outside the horizon ($\tilde{r} > 0$), the whole portion of trapping horizon $\tilde{t}_{\rm TH}^{(+)}$ is past outer for $\tau < \tau_{\rm crit}$, and hence always spacelike, analogous to the FLRW universe filled by a stiff matter, while the trapping horizon $\tilde{t}_{\rm TH}^{(-)}$ is always timelike. Inside the trapping horizon ($\tilde{r} < 0$), $\tilde{t}_{\rm TH}^{(\pm)}$ coincide at $\tilde{r} = \tilde{r}_0$. $\tilde{t}_{\rm TH}^{(-)}$ and a part of $\tilde{t}_{\rm TH}^{(+)}$ near $r \simeq r_0$ are timelike. The other portion of $\tilde{t} = \tilde{t}_{\rm TH}^{(+)}$ changes signature near $\tilde{r} = 0$ into spacelike.

(ii) Trapping horizons occur where $\tilde{R}$ = const surfaces becomes null. The contour curve of circumference radius is spacelike for $\tilde{R}_2 < \tilde{R} < \tilde{R}_1$ (see Fig. 5). As approaching the event horizon, the trapping horizons $\tilde{t}_{\rm TH}^{(\pm)}$ tend to have constant radii $\tilde{R}_\pm$.

(iii) For $\tilde{r} < 0$, the circumference radius $\tilde{R} = [(1 + \tilde{t}\,\tilde{r}) \times (1 + \tilde{r})^3]^{1/4}$ becomes infinitely large as $\tilde{t} \to -\infty$ with $\tilde{r}$ staying constant. We can show, following the same argument in Eq. (4.44), that this is a "past timelike infinity."[5]

Outside the horizon $\tilde{r} > 0$, the $\tilde{R}$ = const ($>\tilde{R}_+$) surfaces are the same as the FLRW cosmology: there exists a spacelike past trapping horizon $\tilde{t}_{\rm TH}^{(+)}(\tilde{r})$, above which $\tilde{R}$ = const surfaces are timelike and below which $\tilde{R}$ = const surfaces are spacelike (see Fig. 10). For $\sqrt{\tau} \equiv 1 < \tilde{R} < \tilde{R}_+$, $\tilde{R}$ = const curves are everywhere spacelike and lie in the future of a critical null curve $\tilde{t} = \tilde{t}_*(\tilde{r})$. For $\tilde{R}_- < \tilde{R} < 1 \equiv \sqrt{\tau}$, $\tilde{R}$ = const curves cross the future trapping horizon $\tilde{t}_{\rm TH}^{(-)}(\tilde{r})$ and change signature. For $\tilde{R} < \tilde{R}_-$, $\tilde{R}$ = const curves are always timelike.

Inside the horizon ($\tilde{r} < 0$), $\tilde{R}$ = const curves are the same as outside for $\tilde{R} < \tilde{R}_-$ and $\sqrt{\tau} \equiv 1 < \tilde{R} < \tilde{R}_+$. Whereas, $\tilde{R}$ = const curves for $\tilde{R} > \tilde{R}_+$ quite differ from those in the outside. They cross the trapping horizons twice.

V. BLACK-HOLE THERMODYNAMICS

Black-hole thermodynamics has been established as rigorous mathematical laws of black holes with Killing horizons [23–30]. Since the three laws of black-hole thermodynamics interrelate the classical gravity, quantum mechanics, and statistical mechanics, they are likely to have a key role toward quantum laws of gravity. Last, we discuss the thermodynamic properties of the present time-dependent black hole.

Since the present spacetime (4.1) possesses a Killing horizon, the thermodynamic laws continue to hold without change. It turned out that the Killing horizon has nonvanishing surface gravities (4.56). However, their values

[5]This is slightly different from the extremal RN geometry, for which it takes an infinite affine time to reach the corresponding point from inside the black hole, but the point is located at the finite circumference radius. The reason why the point in the present spacetime has an infinite circumference radius inside the horizon might be due to the cosmic expansion.

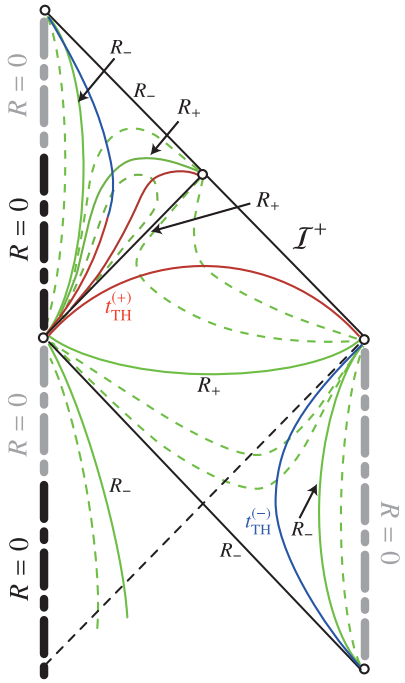

FIG. 10 (color online). A conformal diagram of the black hole in the expanding universe. The curves of $\tilde{R} = \text{const}$ are shown by green lines. Null curve $\tilde{R}_+$ is the future-event horizon, and $\mathcal{I}^+$ is the future null infinity. The trapping horizons $\tilde{t} = \tilde{t}^{(+)}_{\rm TH}(\tilde{r})$ and $\tilde{t} = \tilde{t}^{(-)}_{\rm TH}(\tilde{r})$ are also shown by red and blue lines. The diagram can be extended beyond the upper $\tilde{R}_-$ null curve (possibly with the contracting patch $\tau < 0$ that turns the above figure upside down) in a continuous but nonanalytic manner.

are dependent on the normalization of the Killing field generators of the horizon. Here, we intend to obtain the temperature associated with the time translation in the FLRW universe. To this end, we resort to the laws of trapping horizons. This is a hotly discussed issue in recent years [44,45,48]. Laws of trapping horizons are local extensions of black-hole thermodynamics.

When discussing the dynamical aspects of black holes, a major obstacle for extending the black-hole thermodynamics to a nonstationary setting is how to define a surface gravity. In the case of a spherically symmetric spacetime, a natural time direction is specified by the *Kodama flow* [44,45,54].

Write the spherically symmetric metric as

$$ds^2 = g_{AB}(x)dx^A dx^B + R^2(x)d\Omega_2^2, \tag{5.1}$$

where $g_{AB}(x)$ $(A, B = 1, 2)$ is the two-dimensional Lorentz manifold (M^2, g_{AB}) perpendicular to the metric sphere. The coordinate, x^A, on M^2 corresponds to t and r. Using this coordinate patch, the Kodama vector is defined by [54]

$$K^A = -\epsilon^{AB} D_B R, \tag{5.2}$$

where ϵ_{AB} and D_A are the volume element and the covariant derivative of g_{AB}. We may view K^A as a spacetime vector by $K^\mu = K^A(\partial_A)^\mu$. It follows immediately from the orthogonal property $K^\mu \nabla_\mu R = 0$ that K^μ is divergence free, $\nabla_\mu K^\mu = R^{-2} D_A(R^{-2}K^A) = 0$. Another key property comes from the relation $K^\mu K_\mu = -(\nabla_\mu R)(\nabla^\mu R)$, so that K^μ is timelike (spacelike) in the untrapped (trapped) region, i.e., K^μ defines a preferred timelike direction in the untrapped region, irrespective of the nonstationarity of spacetime. Specifically, the Kodama vector becomes null at the trapping horizon, just as in the same way the Killing vector becomes null at the Killing horizon.

It is enlightening here to look into the relation between K^μ and the Misner-Sharp energy, which is also characteristic of spherically symmetric spacetimes [43]. Inspecting $\nabla_\mu K_\nu = D_A K_B(\nabla_\mu x^A)(\nabla_\nu x^B)$, a simple calculation shows that $\mathcal{G}_{\mu\nu}\nabla^\mu K^\nu = 0$ holds in any spherical spacetimes. Hence we can define a divergence-free vector field $\kappa^2 J^\mu = -\mathcal{G}^\mu{}_\nu K^\nu$, representing an energy current due to the Einstein equations. Integration of J^μ over the volume V with exterior boundary S yields the Misner-Sharp energy $m = -\int_V J^\mu d\Sigma_\mu$. To summarize, the Misner-Sharp energy is a charge associated with the locally conserved current.

As seen above, the Kodama vector in the spherical spacetime plays a role similar to the Killing field in stationary spacetime. One can speculate that laws of trapping horizons are related to an observer along the Kodama flow.

A. Temperature: 0th law

A naïve definition of the surface gravity for the trapping horizon is to replace the Killing field by the Kodama vector in the definition of surface gravity of a Killing horizon. This prescription does not work, since the trapping horizon is not the null surface generated by the Kodama vector. A proposed definition of surface gravity for the trapping horizon [44,45] is given by the "equilibrium part"

$$K^\nu \nabla_{[\nu} K_{\mu]} = \kappa_{\rm TH} K_\mu, \tag{5.3}$$

where the equality is evaluated at the trapping horizon. After some amount of algebra, one finds that the surface gravities of trapping horizons $\tilde{t} = \tilde{t}^{(\pm)}_{\rm TH}$ are given by

$$\tilde{\kappa}^{(+)}_{\rm TH} = \frac{(1+\tilde{r})^6(1+4\tilde{r})^3}{8\tilde{R}_1^9}\left[\frac{4\tilde{r}^2+8\tilde{r}+1}{(1+\tilde{r})^8}\tilde{R}_1^8 - 1\right], \tag{5.4}$$

$$\tilde{\kappa}^{(-)}_{\rm TH} = \frac{(1+\tilde{r})^6(1+4\tilde{r})^3}{8\tilde{R}_2^9}\left[\frac{4\tilde{r}^2+8\tilde{r}+1}{(1+\tilde{r})^8}\tilde{R}_2^8 - 1\right]. \tag{5.5}$$

Taking the event horizon limit $\tilde{r} \to 0$ [see Eqs. (4.30) and (4.31)] in the above equations, we obtain the black-hole temperature

$$T^{(\pm)}_{\rm BH} := \left.\frac{\tilde{\kappa}^{(\pm)}_{\rm TH}}{2\pi Q}\right|_{\tilde{r}\to 0} = \frac{\sqrt{1+4\tau^2}}{16\pi\tau^2\tilde{R}_\pm^5 Q}. \tag{5.6}$$

Comparing this with Eq. (4.56), these are equivalent to

surface gravities associated with a renormalized generator of the horizon,

$$\xi^\mu = \left(\frac{\partial}{\partial \tilde{T}_\pm}\right)^\mu \to \frac{1}{4\tau \tilde{R}_\pm^3}\left(\frac{\partial}{\partial \tilde{T}_\pm}\right)^\mu, \tag{5.7}$$

which coincides with the Kodama vector evaluated on the horizon for the near-horizon metric (4.53).

For the future horizon $\tilde{R}_+$, the temperature $T_{\rm BH}^{(+)}$ takes the maximum value

$$T_{\rm BH(max)}^{(+)} = \frac{3^{-(9/4)}}{2\pi Q} \approx 0.002\,138\,56 Q^{-1} \tag{5.8}$$

at $\tau = \sqrt{3}/2$ for fixed charge. The temperature vanishes in both limits of $\tau \to \infty$ (degenerate horizon) and $\tau \to 0$ (no horizon). The former recovers the result for the extremal RN black hole. The temperature at the past horizon $\tilde{R}_-$, on the other hand, has no maximum value. It monotonically increases to infinity as $\tau \to 0$. $T_{\rm BH}^{(-)}$ is always higher than $T_{\rm BH}^{(+)}$.

B. Energy balance: 1st law

It is a widely accepted criterion that a well-defined energy should satisfy an energy balance law. The Misner-Sharp energy indeed fulfills this, as in Eq. (4.17). We can rewrite each term in this equation into a more recognizable form. Defining 2D quantities,

$$P_{\rm eff} = -\tfrac{1}{2}T^A{}_A, \qquad \psi_A = T_{AB}D^B R + P D_A R, \tag{5.9}$$

and making use of the Einstein equations, one arrives at the *unified first law* [45],

$$D_A m = A\psi_A + P_{\rm eff} D_A V, \tag{5.10}$$

where $A = 4\pi R^2$ and $V = \frac{4\pi}{3}R^3$ denote the area and volume of the metric sphere. This equation illustrates that the mass variation is supplied by an injection of energy current and the external work term. The expression of ψ_A is comparatively messy, but it is straightforward to obtain.

Projecting Eq. (5.10) along the generator, $\zeta^\mu = \zeta^A(\partial_A)^\mu$, of the trapping horizon and noticing the fact that $\zeta^\mu \nabla_\mu (m/R) = 0$, one obtains

$$A\zeta^A \psi_A = \frac{\kappa_{\rm TH}}{8\pi}\zeta^A D_A A. \tag{5.11}$$

This is an energy balance law of a trapping horizon (see [43,45] for a detailed derivation). Here, along the trapping horizon with $\theta_+ = 0$, ζ^A is obtained as $\zeta^A = \pm\epsilon^{AB}D_B\theta_+$ (where the sign should be appropriately chosen in such a way that it is outgoing in the spacelike case or future directed in the timelike case).

Using Einstein's equations, we find that the surface gravity is expressed in terms of the Misner-Sharp energy and the pressure as

$$\kappa_{\rm TH} = \frac{m}{R^2} - 4\pi R P_{\rm eff}, \tag{5.12}$$

where equality is understood at the trapping horizon. This is the Newtonian analog definition of acceleration.

C. Entropy: 2nd law

It follows from the first law of a trapping horizon that we can identify the entropy by one-quarter of the area of the trapping horizon, i.e., it is in accordance with the "Bekenstein-Hawking formula,"

$$S_{\rm TH}^{(+)} = \frac{A_1}{4G} = \frac{\pi R_1^2}{G}, \qquad S_{\rm TH}^{(-)} = \frac{A_2}{4G} = \frac{\pi R_2^2}{G}. \tag{5.13}$$

Taking the event horizon limit (4.30) or (4.31), we recover the well-known result [25,27]

$$S_{\rm BH}^{(\pm)} = \frac{A_{\rm BH}^{(\pm)}}{4G} = \frac{\pi Q^2}{2G\tau}(\pm 1 + \sqrt{1 + 4\tau^2}). \tag{5.14}$$

In the limit $\tau \to \infty$ with fixed charge, the above entropy reduces to that of the extremal RN black hole, $S_{\rm BH}^{(\pm)} = \pi Q^2/G$.

VI. CONCLUDING REMARKS

In this paper, we have had a thorough discussion about the causal structure and physical properties of the spacetime derived from intersecting M-branes. We have found that the solution indeed describes a black hole embedded in the FLRW cosmology filled with fluid obeying the stiff equation of state. The global causal structure is displayed in Figs. 9 and 10. Since the solution is approximated by the extreme RN solution near the throat and the flat FLRW universe with $P = \rho$ at infinity, one might first envisage that the causal structure is obtainable by patching these two limiting spacetimes. That is to say, according to our first intuition, one might have expected that spacetime should possess a spacelike big-bang singularity at $t = 0$, there should exist a degenerate event horizon, and the timelike singularity should appear only inside the hole. However, our careful analysis revealed that the global causal structure is completely different from the above rough estimate.

Our solution satisfies the dominant energy condition, so that the energy densities are always positive, absolute values of principal pressures do not exceed the energy density for respective fluids, and the energy flux current is always causal. This desirable property is not seen in the solutions found in the literature. Hence the results presented in this paper open up new avenues for further research on black holes surrounded by usual matters in the expanding universe from a higher-dimensional point of view. Our solution, however, may not have a direct astrophysical relevance because of nonzero electromagnetic charge. The charge is probably also responsible for the timelike singularity $t = t_s(r)$ outside the horizon. The timelike singularity does not develop as the big-bang sin-

gularity in the usual FLRW cosmology with fluid $P = w\rho(-1 \leq w \leq 1)$. Unfortunately, the construction of a black-hole solution without charge may be beyond the intersecting brane picture.

In the process for obtaining the global structure, we gave a coherent description concerning the trapping horizons. The main idea on which our discussion is based is that the trapping horizons reflect the physical situations of marginal surfaces on which either of the expansions of the light ray vanishes. This local character enables us to relate it to the curvature singularity and the Misner-Sharp energy. A more important belief to which we resort is that the trapping horizon with negative outgoing expansion does not occur outside the horizon. The present spacetime indeed has this property (except in the neighborhood of singularity). We confirm the infinite redshift (blueshift) surface as a black-hole horizon (white-hole horizon in a quoted sense) combining the analysis of near-horizon geometry and the behaviors of null geodesics.

It was somewhat surprising that the solution admits a nondegenerate Killing horizon. The Killing horizon is usually associated with symmetry of time translation and angular rotation. The black hole remains the same size and fails to grow, although the black hole is surrounded with fluid. This characteristic property may be ascribed to the fact that the 11D solution was supersymmetric in the static limit. Although the dynamically brane intersecting solution breaks supersymmetry, it still maintains a part of the BPS characters. The same takes place in the Kastor-Traschen black hole.

In this paper, we have taken a particular notice on the solution, whose 11D ''oxidized'' solution has four kinds of harmonics of spherical symmetry. A more general nonspherical spacetime is of course more complicated. Still, the profound understanding of the spherically symmetric case will be of substantial aid in exposing more complex structures of dynamical black holes.

ACKNOWLEDGMENTS

We would like to thank Gary W. Gibbons, Hideki Maeda, Nobuyoshi Ohta, and Harvey S. Reall for valuable comments and discussions. K. M. acknowledges the hospitality of DAMTP and the Centre for Theoretical Cosmology, Cambridge University, during his stay in September, 2009. This work was partially supported by the Grant-in-Aid for Scientific Research Fund of the JSPS (No. 19540308) and for the Japan-U.K. Joint Research Project, and by the Waseda University Grants for Special Research Projects.

APPENDIX A: INTERSECTING BRANE AND BLACK HOLES

In this Appendix, we consider an intersecting brane system in the 11D supergravity theory, which is expected to be an effective field theory of M theory. We discuss how to obtain the 4D effective action and produce solutions in the 4D spacetime. We intend to consider M-branes, for which the Chern-Simons term $F \wedge F \wedge A$ has no contribution. Hence, it suffices in our setup to concentrate on the following 11D effective action:

$$\mathcal{S} = \frac{1}{2\kappa_{11}^2}\int d^{11}X\sqrt{-g_{11}}\Big[\mathcal{R}_{11} - \sum_A \frac{1}{2(p_A+2)!} \times (\mathcal{F}_{p_A+2})^2\Big]. \tag{A1}$$

Here, A denotes the type of branes with which the Abelian $(p_A + 2)$-form field F_{p_A+2} is coupled, and p_A ($= 2$ or 5) is the dimensions of branes.

Once the 11D brane configuration is given, the 4D solution is derivable via the standard toroidal compactification. We shall analyze intersecting brane systems involving four charges, which is needed to find a 4D maximally charged (supersymmetric or nonsupersymmetric) black hole with regular event horizon. We can construct two kinds of such a configuration: the M2-M2-M5-M5 and the M2-M5-W-KK systems. As a concrete example, we focus our attention on the M2-M2-M5-M5 intersecting brane system. Compatibility with 11D supergravity equations of motion determines respective brane codimensions, which is given by Table I.

There appear four charges $(Q_2, Q_{2'}, Q_5, Q_{5'})$ associated with the corresponding four branes. In the static spacetime, we have the following intersecting brane solution:

$$\begin{aligned} ds^2 = {} & H_2^{1/3}H_{2'}^{1/3}H_5^{2/3}H_{5'}^{2/3}[-H_2^{-1}H_{2'}^{-1}H_5^{-1}H_{5'}^{-1}dt^2 \\ & + H_5^{-1}H_{5'}^{-1}(dy_1^2 + dy_2^2 + dy_3^2) + H_5^{-1}H_2^{-1}dy_4^2 \\ & + H_5^{-1}H_{2'}^{-1}dy_5^2 + H_2^{-1}H_{5'}^{-1}dy_6^2 + H_{2'}^{-1}H_{5'}^{-1}dy_7^2 \\ & + (dr^2 + r^2 d\Omega_2^2)], \end{aligned} \tag{A2}$$

where H_A are harmonics on the three Euclidean space $(ds_3^2 = dr^2 + r^2 d\Omega_2^2)$. One can see immediately that the directions involving inverse H_A for the metric in the square bracket correspond to the dimensions to which the A-brane belong.

If one toroidally compactifies the common 7D world volume of branes, a 4D solution is obtained. Rewriting the 11D metric as

TABLE I. M2-M2-M5-M5 brane system. The circles describe which dimensions are filled by the corresponding branes.

	0	1	2	3	4	5	6	7	8	9	10
M5	∘	∘	∘	∘	∘	∘					
M5	∘	∘	∘	∘			∘	∘			
M2	∘				∘		∘				
M2	∘					∘		∘			

$$ds^2 = \prod_{i=1}^{7} b_i^{-1} \times ds_4^2 + \sum_{i=1}^{7} b_i^2 dy_i^2, \tag{A3}$$

where

$$b_1^2 = b_2^2 = b_3^2 = \left(\frac{H_2 H_{2'}}{H_5 H_{5'}}\right)^{1/3}, \tag{A4}$$

$$\begin{aligned} b_4^2 &= \left(\frac{H_{2'} H_{5'}^2}{H_2^2 H_5}\right)^{1/3}, \qquad b_5^2 = \left(\frac{H_2 H_{5'}^2}{H_{2'}^2 H_5}\right)^{1/3}, \\ b_6^2 &= \left(\frac{H_{2'} H_5^2}{H_2^2 H_{5'}}\right)^{1/3}, \qquad b_7^2 = \left(\frac{H_2 H_5^2}{H_{2'}^2 H_{5'}}\right)^{1/3}, \end{aligned} \tag{A5}$$

and compactifying y_i coordinates ($i = 1, \ldots, 7$), the 4D solution in the Einstein frame is given by

$$ds_4^2 = -\Xi dt^2 + \frac{1}{\Xi}(dr^2 + r^2 d\Omega_2^2), \tag{A6}$$

where

$$\Xi = (H_2 H_{2'} H_5 H_{5'})^{-1/2}. \tag{A7}$$

If we assume that harmonics H_A's are spherically symmetric, i.e.,

$$\begin{aligned} H_2 &= 1 + \frac{Q_2}{r}, \qquad H_5 = 1 + \frac{Q_5}{r}, \\ H_{2'} &= 1 + \frac{Q_{2'}}{r}, \qquad H_{5'} = 1 + \frac{Q_{5'}}{r}, \end{aligned} \tag{A8}$$

we find a static extreme black-hole solution in four dimensions. Here, Q_A's represent the brane charges. If all charges vanish, both of the 11D and 4D solutions are trivial. The extension of the harmonic functions H_A as discussed in Appendix B gives a multi-black-hole system.

Generalizing this solution to the time-dependent one, we find that only one brane among four can be time dependent under the metric ansatz assumed in [20]. The intersecting brane metric is still given by Eq. (A2). The field equations require that the time dependence is linear, i.e., the metric functions in the spherically symmetric case are given by

$$\begin{aligned} H_T &= \frac{t}{t_0} + \frac{Q_T}{r}, \qquad H_S = 1 + \frac{Q_S}{r}, \\ H_{S'} &= 1 + \frac{Q_{S'}}{r}, \qquad H_{S''} = 1 + \frac{Q_{S''}}{r}, \end{aligned} \tag{A9}$$

where t_0 is a constant with dimension of time. T and S, S', S'' denote one time-dependent brane and three static branes, respectively. Any one of M2, M2′, M5, and M5′ branes can have time dependence. This gives a black hole in the expanding universe in four dimensions, which we discuss in this paper. It is also extended to a multi-black-hole system (see Appendix B). If all brane charges are set to zero, the 11D solution is the Kasner solution describing a homogeneous but anisotropic vacuum universe, whereas the 4D solution reduces to the flat FLRW cosmology.

Since we know the 11D action (A1), assuming the brane configuration shown in Table I and compactifying the spatial directions as (A3), we can derive the effective 4D action, which gives the present time-dependent solutions, as follows.

The scales of extra dimensions b_i ($i = 1, \ldots, 7$) behave as scalar fields in 4D spacetime, i.e., the effective action of the gravity sector is

$$\begin{aligned} \mathcal{S}_4(g, b_i) = \int d^4x \sqrt{-g} \Big\{ \frac{1}{2\kappa^2} R - \frac{1}{4} \Big[\Big(\nabla \sum_{i=1}^{7} \ln b_i \Big)^2 \\ + 2 \sum_{i=1}^{7} (\nabla \ln b_i)^2 \Big] \Big\}. \end{aligned} \tag{A10}$$

Although we compactify seven dimensions, we have only four branes. Hence the degrees of freedom are maximally 4. This can be affirmed by writing down the kinetic term of the scalar fields in terms of harmonic functions H_A as

$$\begin{aligned} \frac{1}{4}\Big[\Big(\nabla \sum_{i=1}^{7} \ln b_i \Big)^2 + 2 \sum_{i=1}^{7} (\nabla \ln b_i)^2 \Big] &= \frac{1}{16} [3\{(\nabla \ln H_2)^2 + (\nabla \ln H_{2'})^2 + (\nabla \ln H_5)^2 + (\nabla \ln H_{5'})^2\} \\ &\quad - 2(\nabla \ln H_2 \cdot \nabla \ln H_{2'} + \nabla \ln H_5 \cdot \nabla \ln H_{5'}) - 2(\nabla \ln H_2 \cdot \nabla \ln H_5 + \nabla \ln H_2 \cdot \nabla \ln H_{5'} \\ &\quad + \nabla \ln H_{2'} \cdot \nabla \ln H_5 + \nabla \ln H_{2'} \cdot \nabla \ln H_{5'})] \\ &= \frac{1}{16} [(\nabla \ln(H_2/H_{2'}))^2 + (\nabla \ln(H_5/H_{5'}))^2 + (\nabla \ln(H_2/H_5))^2 + (\nabla \ln(H_2/H_{5'}))^2 \\ &\quad + (\nabla \ln(H_{2'}/H_5))^2 + (\nabla \ln(H_{2'}/H_{5'}))^2] \\ &= \frac{\kappa^2}{2} \sum_{A<B} (\nabla \phi_{AB})^2, \end{aligned} \tag{A11}$$

where

$$\kappa\phi_{AB} = \frac{1}{2\sqrt{2}} \ln\left(\frac{H_A}{H_B}\right), \tag{A12}$$

denotes the "scalar field mixing" term.

Supposing that all charges are equal ($Q_2 = Q_{2'} = Q_5 = Q_{5'} \equiv Q$) as in the main text, it follows that $\phi_{SS'}$, $\phi_{S'S''}$, and $\phi_{SS''}$ are trivial, and ϕ_{TS}, $\phi_{TS'}$, and $\phi_{TS''}$ are the same. As a result only a single scalar field Φ survives, which is normalized from (A11) as

$$\kappa\Phi = \sqrt{3}\kappa\phi_{TS} = \frac{\sqrt{3}}{2\sqrt{2}} \ln\left(\frac{H_T}{H_S}\right).$$

This is identical to Eq. (3.8).

Next we reduce the 11D form-field sector as follows: the M2 and M5 branes couple to four-form and its dual seven-form field, respectively. Hence the effective action of the form fields is reduced to four dimensions as

$$\begin{aligned}\frac{1}{2\kappa^2}\sqrt{-g_{11}}\sum_A \frac{1}{2(p_A+2)!}(\mathcal{F}_{p_A+2})^2 &= \left(\prod_i b_i^{-1}\right)^2 \prod_i b_i \sqrt{-g}\left(\prod_i b_i^{-1}\right)^{-2} \frac{g^{\mu\rho}g^{\nu\sigma}}{8\pi}[F^{(2)}_{\mu\nu}F^{(2)}_{\rho\sigma}b_4^{-2}b_6^{-2} + F^{(2')}_{\mu\nu}F^{(2')}_{\rho\sigma}b_5^{-2}b_7^{-2} \\ &\quad + F^{(5)}_{\mu\nu}F^{(5)}_{\rho\sigma}b_1^{-2}b_2^{-2}b_3^{-2}b_4^{-2}b_5^{-2} + F^{(5')}_{\mu\nu}F^{(5')}_{\rho\sigma}b_1^{-2}b_2^{-2}b_3^{-2}b_6^{-2}b_7^{-2}] \\ &= \sqrt{-g}\frac{1}{4}\left[\left(\frac{H_T}{H_S}\right)^{3/2}(F^{(T)}_{\mu\nu})^2 + 3\left(\frac{H_T}{H_S}\right)^{-1/2}(F^{(S)}_{\mu\nu})^2\right],\end{aligned} \tag{A13}$$

where we set

$$(F^{(A)}_{\mu\nu})^2 = \frac{2\pi}{\kappa^2(p_A+2)!}(\mathcal{F}_{p_A+2})^2. \tag{A14}$$

This ansatz is consistent with our result (3.11) for the Maxwell fields, because the electric potential of the four-form field in 11D is given by $\mathcal{A}_0^{(A)} = 1/H_A + a^{(A)}(t)$, where $a^{(A)}(t)$ is an arbitrary function of t, which comes from a gauge freedom. As a result, we obtain the effective 4D action for the form-field sector as

$$\begin{aligned}\mathcal{S}_4(F) = \frac{1}{16\pi}\int d^4x\sqrt{-g}[&e^{\mp\sqrt{6}\kappa\Phi}(F^{(T)}_{\mu\nu})^2 \\ &+ 3e^{\pm\sqrt{6}\kappa\Phi/3}(F^{(S)}_{\mu\nu})^2],\end{aligned} \tag{A15}$$

which is the same as Eq. (3.2).

In the static case with equal charges, the 4D solution (A6) with (A8) corresponds to an extreme RN black hole (which is indeed a solution in the Einstein-Maxwell system). While for the time-dependent case with equal charges (A9), it describes a black hole in the FLRW universe which we have established in the body of the present paper.

APPENDIX B: MULTIBLACK HOLES IN THE TIME-DEPENDENT UNIVERSE

Writing $H_T = t/t_0 + \bar{H}_T$, $H_S = 1 + \bar{H}_S$, and so on, the 11D supergravity equations of motion require the functions $\bar{H}_A$ ($A = T, S, S'$, and S'') to be arbitrary harmonics on flat three space. Hence, just by replacing the monopole term Q_A/r by multicenter harmonics, we obtain a collection of black holes in a dynamical background. To be specific, we have

$$\bar{H}_A = \sum_i^N \frac{Q_i^{(A)}}{|\boldsymbol{r} - \boldsymbol{r}_i^{(A)}|}, \tag{B1}$$

where the constants $\boldsymbol{r}_i^{(A)}$ and $Q_i^{(A)}$ (> 0) correspond to the loci and the charges of ith black hole associated with A-branes, respectively. The linear term $(\boldsymbol{a}_i \cdot \boldsymbol{r}_i)$ has been dropped by the asymptotic boundary conditions at infinity. In the case of three equal harmonics $\bar{H}_S = \bar{H}_{S'} = \bar{H}_{S''}$, this metric solves the field equations of Einstein-Maxwell-dilaton system (3.2) if the dilaton and U(1)-gauge potentials are given by (3.8) and (3.11).

Near each mass point (with t being finite) $\boldsymbol{r}_i^{(A)}$, there exists an infinite throat as in the single mass case discussed in the body of the text. Far from the throat, on the other hand, the solution tends to an FLRW universe filled by a stiff matter.

As in the case of the Kastor-Traschen solution [37,38], this spacetime is expected to describe a collision of black holes provided the background universe is contracting ($t_0 < 0$). Since each black hole is ignorant of others, i.e., the gravitational and electromagnetic forces between black holes are balanced, the collision occurs by a brute-force method responsible for the background contracting universe. The difference from the Kastor-Traschen case lies in the fact that the background universe obeys the power-law contraction $a \propto \bar{t}^{1/3}$, so our discussion parallels [18] in which colliding D3 branes were discussed in detail.

Let us start with the negative time $t < 0$ and run time forward. Since the $t = 0$ surface is again nonsingular, the universe continues to shrink for positive values of t until the singularity $H_T = 0$ is reached. Specifically, the metric continues to exist inside the domain, D_t, bounded by the level set $\bar{H}_T = t/(-t_0)$. It then follows that at small positive t, the domain D_t is a large connected volume contain-

ing all black holes. As time passes, the domain D_t continues to contract and tends to split into disconnected pieces containing each mass point $\boldsymbol{r}_i^{(A)}$. This means that black holes scatter off rather than coalesce, and the universe is bounded by curvature singularity at $H_T = 0$.

The multiple black-hole solution (B1) is to be compared with the Kastor-Traschen solution,

$$ds^2 = -H^{-2}dt^2 + H^2 d\boldsymbol{r}^2, \tag{B2}$$

with $\kappa F = d(H^{-1}) \wedge dt$, and

$$H = \frac{t}{t_0} + \bar{H}, \qquad \bar{H} := \sum_i^N \frac{Q_i}{|\boldsymbol{r} - \boldsymbol{r}_i|}. \tag{B3}$$

This is an exact solution of the Einstein-Maxwell-$\Lambda(\equiv 3/t_0^2)$ system. The distinction between our spacetime and the Kastor-Traschen solution is essentially only the power of the lapse function, where divergence of lapse corresponds to the curvature singularity for each solution. The exponent is closely associated with the number of branes and a more general class of solutions is available. Further detailed analysis will be reported elsewhere [55].

APPENDIX C: 5D TIME-DEPENDENT BLACK HOLES

As proved in [20], a 5D time-dependent black-hole solution is also obtained from the M2-M2-M2 and M2-M5-W intersecting brane systems. Let us discuss the former case. As in the static counterparts, we need only three nontrivial charges to obtain a black-hole solution. The 5D metric in the Einstein frame reads

$$ds_5^2 = -\Xi^2 dt^2 + \Xi^{-1}(dr^2 + r^2 d\Omega_3^2), \tag{C1}$$

with

$$\Xi = (H_T H_S H_{S'})^{-1/3}. \tag{C2}$$

Here we have introduced

$$H_T = \frac{t}{t_0} + \frac{Q_T}{r^2}, \qquad H_S = 1 + \frac{Q_S}{r^2}, \qquad H_{S'} = 1 + \frac{Q_{S'}}{r^2}, \tag{C3}$$

to denote the harmonics in the flat 4D space. Q_T and Q_S, $Q_{S'}$ are charges of one time-dependent and two remaining static M2 branes, respectively. The lapse function Ξ takes a relatively simple form compared to the 4D metric (2.2).

Assuming $t/t_0 > 0$ and transforming to the new time coordinate $\bar{t}$ given by

$$\frac{\bar{t}}{\bar{t}_0} = \left(\frac{t}{t_0}\right)^{2/3} \quad \text{with} \quad \bar{t}_0 = \frac{3t_0}{2}, \tag{C4}$$

the solution (C1) is cast into the form,

$$ds_5^2 = -\bar{\Xi}^2 d\bar{t}^2 + \frac{a^2}{\bar{\Xi}}(dr^2 + r^2 d\Omega_2^3), \tag{C5}$$

where

$$\bar{\Xi} = (\bar{H}_T H_S H_{S'})^{-1/3}, \tag{C6}$$

$$a = (\bar{t}/\bar{t}_0)^{1/4}, \tag{C7}$$

with

$$\bar{H}_T = 1 + \frac{Q_T}{a^6 r^2}. \tag{C8}$$

The expansion law with (C7) is again identical to that of the 5D universe with a stiff matter. The limit of $r \to 0$ with keeping t finite gives the same throat geometry of the 5D extreme RN black hole. According to the detailed argument laid out in the main text, we may regard this solution as a black hole in the expanding universe.

For the case in which $Q_T = Q_S = Q_{S'} =\equiv Q$, the 5D metric is an exact solution of the Einstein-Maxwell-dilaton system whose action is given by

$$\mathcal{S} = \int d^4x\sqrt{-g}\Big[\frac{1}{2\kappa^2}\mathcal{R} - \frac{1}{2}(\nabla\Phi)^2 - \frac{1}{16\pi}\sum_A e^{\lambda_A \kappa\Phi}(F_{\mu\nu}^{(A)})^2\Big], \tag{C9}$$

if the dilaton is given by

$$\Phi = \frac{1}{\sqrt{3}}\ln\left(\frac{H_T}{H_S}\right), \tag{C10}$$

and the electromagnetic fields take the form,

$$\kappa A_0^{(T)} = \sqrt{2\pi}\frac{1}{H_T}, \qquad \kappa A_0^{(S)} = \kappa A_0^{(S')} = \sqrt{2\pi}\left(\frac{1}{H_S} - 1\right), \tag{C11}$$

with coupling constants

$$\lambda_T = \frac{4}{\sqrt{3}}, \qquad \lambda_S = \lambda_{S'} = -\frac{2}{\sqrt{3}}. \tag{C12}$$

After short calculations, we find the following results. The horizon radii are given by

$$R_\pm^3 = \frac{Q^{3/2}}{\tau}(\sqrt{1 + 16\tau^2} \pm 1), \tag{C13}$$

where

$$\tau^2 = \frac{t_0^2}{Q}. \tag{C14}$$

R_+ and R_- correspond to the future-event horizon and the past-event horizon, respectively. The Carter-Penrose diagram is quite similar to that in 4D, although there exist minor differences.

The surface gravities are found to be

$$\kappa_{\mathrm{BH}}^{(\pm)} = \frac{\sqrt{1 + 16\tau^2}}{12\tau^2 Q^{1/2}\tilde{R}_\pm^7}. \tag{C15}$$

The temperature of the future-event horizon $[T_{\mathrm{TH}}^{(\pm)} = \kappa_{\mathrm{BH}}^{(\pm)}/(2\pi)]$ vanishes in both the limits of $\tau \to 0$ and of

$\tau \to \infty$, just as the 4D black hole. The maximum temperature is given by

$$T^{(+)}_{\mathrm{BH(max)}} = \frac{4\sqrt[12]{13}\sqrt[3]{1+\sqrt{13}}\sqrt{62+14\sqrt{13}}}{\pi(6+\sqrt{62+14\sqrt{13}})^{7/3}Q^{1/2}} \approx 0.039\,546\,5Q^{-1/2}, \tag{C16}$$

at

$$\tau = \frac{\sqrt[4]{13}(\sqrt{13}+1)}{24} \approx 0.364\,381. \tag{C17}$$

[1] G. W. Gibbons and K. Maeda, Nucl. Phys. **B298**, 741 (1988).
[2] A. Strominger and C. Vafa, Phys. Lett. B **379**, 99 (1996).
[3] J. M. Maldacena, arXiv:hep-th/9607235.
[4] K. i. Maeda and M. Tanabe, Nucl. Phys. **B738**, 184 (2006).
[5] R. Güven, Phys. Lett. B **276**, 49 (1992).
[6] R. Argurio, F. Englert, and L. Houart, Phys. Lett. B **398**, 61 (1997).
[7] N. Ohta and T. Shimizu, Int. J. Mod. Phys. A **13**, 1305 (1998).
[8] I. Y. Aref'eva, M. G. Ivanov, and I. V. Volovich, Phys. Lett. B **406**, 44 (1997).
[9] N. Ohta, Phys. Lett. B **403**, 218 (1997).
[10] H. Lu, C. N. Pope, E. Sezgin, and K. S. Stelle, Nucl. Phys. **B456**, 669 (1995).
[11] H. Lu, S. Mukherji, and C. N. Pope, Int. J. Mod. Phys. A **14**, 4121 (1999).
[12] H. Lu, S. Mukherji, C. N. Pope, and K. W. Xu, Phys. Rev. D **55**, 7926 (1997).
[13] L. Randall and R. Sundrum, Phys. Rev. Lett. **83**, 3370 (1999); **83**, 4690 (1999).
[14] P. Binetruy, C. Deffayet, and D. Langlois, Nucl. Phys. **B565**, 269 (2000); T. Shiromizu, K. Maeda, and M. Sasaki, Phys. Rev. D **62**, 024012 (2000).
[15] P. Kraus, J. High Energy Phys. 12 (1999) 011.
[16] D. Ida, J. High Energy Phys. 09 (2000) 014.
[17] J. Khoury, B. A. Ovrut, P. J. Steinhardt, and N. Turok, Phys. Rev. D **64**, 123522 (2001).
[18] G. W. Gibbons, H. Lu, and C. N. Pope, Phys. Rev. Lett. **94**, 131602 (2005).
[19] W. Chen, Z. W. Chong, G. W. Gibbons, H. Lu, and C. N. Pope, Nucl. Phys. **B732**, 118 (2006).
[20] K. Maeda, N. Ohta, and K. Uzawa, J. High Energy Phys. 06 (2009) 051.
[21] B. Carter, *Black Hole Equilibrium States in Black Holes*, edited by C. DeWitt and J. DeWitt (Gordon and Breach, New York, 1973).
[22] S. W. Hawking and G. F. R. Ellis, *The Large Scale Structure of Space-time* (Cambridge University Press, Cambridge, England, 1973).
[23] D. J. Bekenstein, Phys. Rev. D **7**, 2333 (1973).
[24] J. M. Bardeen, B. Carter, and S. W. Hawking, Commun. Math. Phys. **31**, 161 (1973).
[25] S. W. Hawking, Commun. Math. Phys. **43**, 199 (1975); **46**, 206(E) (1976).
[26] R. M. Wald, Commun. Math. Phys. **45**, 9 (1975).
[27] R. M. Wald, Phys. Rev. D **48**, R3427 (1993).
[28] V. Iyer and R. M. Wald, Phys. Rev. D **50**, 846 (1994).
[29] V. Iyer and R. M. Wald, Phys. Rev. D **52**, 4430 (1995).
[30] S. Gao and R. M. Wald, Phys. Rev. D **64**, 084020 (2001).
[31] A. Einstein and E. G. Straus, Rev. Mod. Phys. **17**, 120 (1945).
[32] F. Kottler, Ann. Phys. (Leipzig) **56**, 410 (1918).
[33] D. R. Brill and S. A. Hayward, Classical Quantum Gravity **11**, 359 (1994).
[34] J. Sultana and C. C. Dyer, Gen. Relativ. Gravit. **37**, 1347 (2005).
[35] G. C. McVittie, Mon. Not. R. Astron. Soc. **93**, 325 (1933).
[36] B. C. Nolan, Phys. Rev. D**58**, 064006 (1998); Classical Quantum Gravity **16**, 1227 (1999); **16**, 3183 (1999).
[37] D. Kastor and J. Traschen, Phys. Rev. D **47**, 5370 (1993).
[38] D. R. Brill, G. T. Horowitz, D. Kastor, and J. H. Traschen, Phys. Rev. D **49**, 840 (1994).
[39] J. B. Hartle and S. W. Hawking, Commun. Math. Phys. **26**, 87 (1972).
[40] H. K. Kunduri, J. Lucietti, and H. S. Reall, Classical Quantum Gravity **24**, 4169 (2007).
[41] C. W. Misner and D. H. Sharp, Phys. Rev. **136**, B571 (1964).
[42] S. A. Hayward, Phys. Rev. D **53**, 1938 (1996).
[43] H. Maeda and M. Nozawa, Phys. Rev. D **77**, 064031 (2008).
[44] M. Nozawa and H. Maeda, Classical Quantum Gravity **25**, 055009 (2008).
[45] S. A. Hayward, Classical Quantum Gravity **15**, 3147 (1998).
[46] M. Nozawa and H. Maeda, Classical Quantum Gravity **23**, 1779 (2006).
[47] R. Penrose, Phys. Rev. Lett. **14**, 57 (1965).
[48] S. A. Hayward, Phys. Rev. D **49**, 6467 (1994).
[49] S. Hollands and A. Ishibashi, Commun. Math. Phys. **291**, 443 (2009).
[50] H. Saida, T. Harada, and H. Maeda, Classical Quantum Gravity **24**, 4711 (2007).
[51] K. C. K. Chan, J. H. Horne, and R. B. Mann, Nucl. Phys. **B447**, 441 (1995).
[52] S. S. Yazadjiev, Classical Quantum Gravity **22**, 3875 (2005).
[53] I. Racz and R. M. Wald, Classical Quantum Gravity **9**, 2643 (1992).
[54] H. Kodama, Prog. Theor. Phys. **63**, 1217 (1980).
[55] G. W. Gibbons and K. Maeda, arXiv:0912.2809.